Computational models, algorithms & computer codes in accelerator physics

Valentin Ivanov

Stanford Linear Accelerator Center

23 February 2006

Contents

- Introduction
- The areas of activity
- Types of the problems
- Stationary problems (Scalar Fields)
- F/T-domain Electromagnetism (Vector Fields)
- Beam Dynamics & Image Electron Optics
- Optimization & Structural Synthesis

Physical Electronics

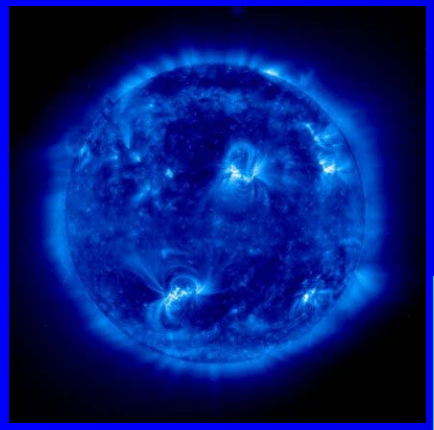

Fokker-Plank equation

$$\frac{\partial f_i}{\partial t} + \vec{v}\frac{\partial f_i}{\partial \vec{r}} + \frac{\vec{F}_i}{M_i}\frac{\partial f_i}{\partial \vec{v}} = \left(\frac{\partial f_i}{\partial t}\right)_c + S_i \ ,$$

Particle Tracking model

$$\dot{\vec{P}}_i = q_i\left\{\vec{E}(\vec{r},t) + \frac{1}{c}\left[\vec{v}\times\vec{H}(\vec{r},t)\right]\right\} - \nabla U_i(\vec{r},\vec{v},t) + \nabla \dot{U}_i,$$

$$\dot{\vec{R}}_i = \frac{\vec{P}_i}{M_i}\left(1 + \frac{P_i^2}{M_i^2 c^2}\right)^{-1/2} .$$

Plasma Physics

Accelerator Physics (vacuum electronics)

$$rot \quad \vec{E} = -\frac{\partial \vec{B}}{\partial t},$$

$$rot \quad \vec{H} = \frac{\partial \vec{D}}{\partial t} + \vec{j}_0 + \sum_i q_i n_i \vec{V}_i,$$

$$div \quad \vec{D} = \frac{\rho}{\varepsilon_0} + \frac{1}{\varepsilon_0}\sum_i q_i n_i,$$

$$div \quad \vec{B} = 0.$$

$$\dot{\rho} + div \quad \vec{j} = 0.$$

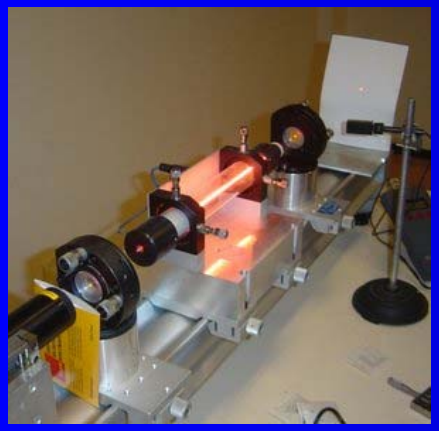

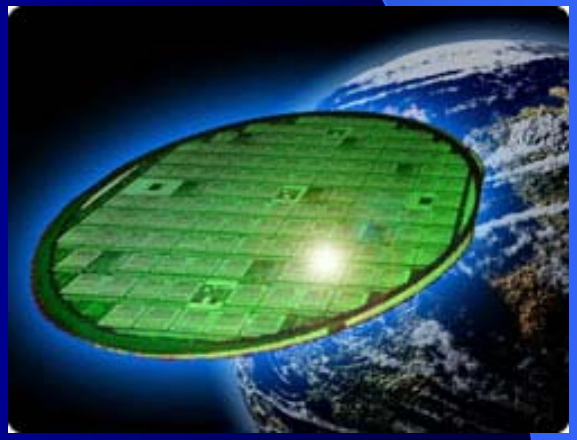

Laser Physics (non linear optics)

Semiconductor micro electronics

The areas of activity

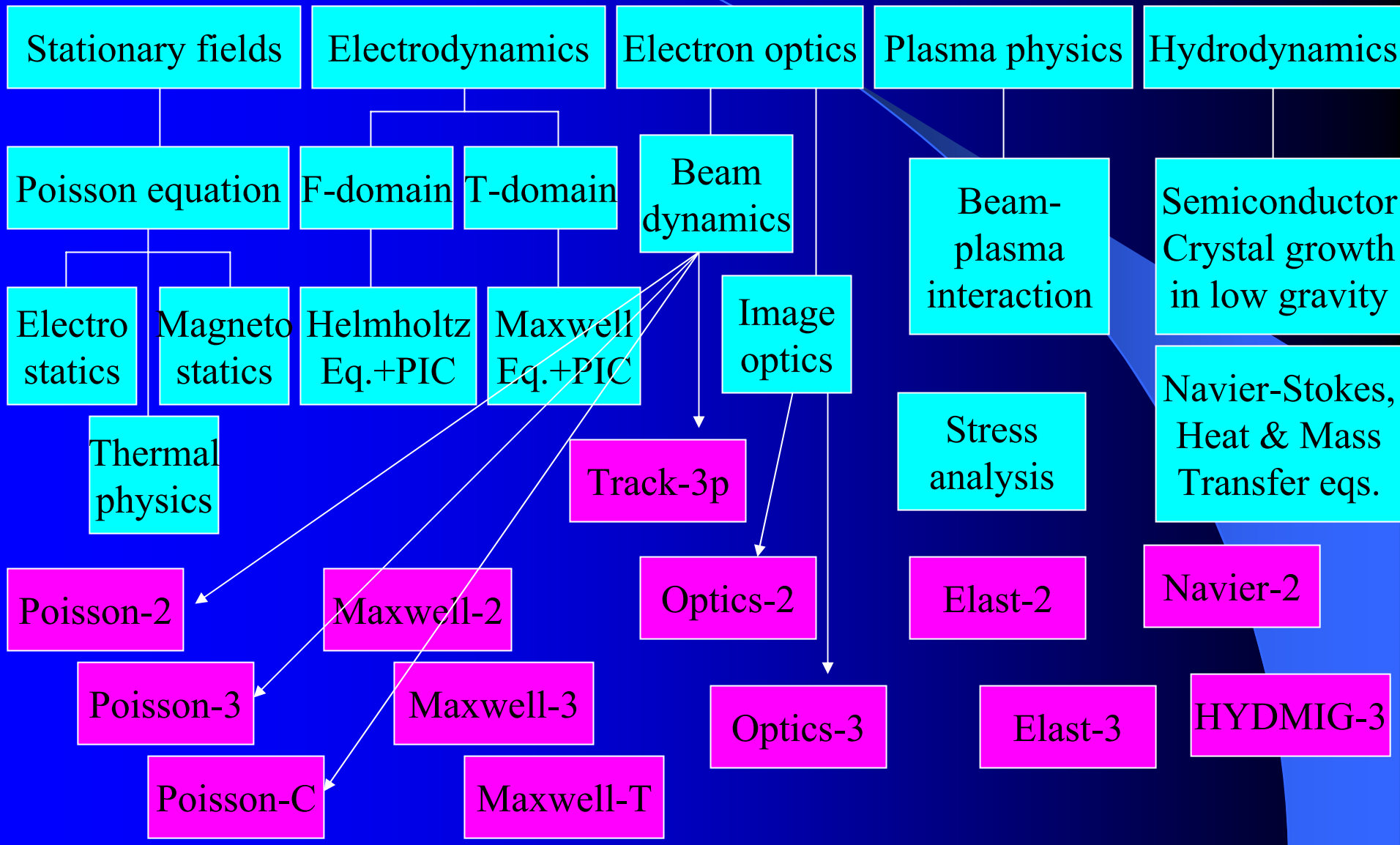

Types of the Design Problems

- Field & particle Analysis
- Parametric Optimization
- Structural Synthesis
- Tolerance Analysis

Comparative features of different numerical methods

Method	FDM	FEM	BEM
Matrix Solver	Iterative	Iterative, Direct	Direct
Matrix dimension 2D 3D	 10^4 10^6	 10^3 10^4 - 10^5	 10^2 10^2-10^3
Advantages	• Uniform operations; • Simple structure of the mesh	• Flexible boundary-fitted mesh • Analytical integration over the element's volume	1. High accuracy; 2. Open boundary; 3. High-order derivatives; 4. Edge singularity 5. External asymptotic;
Disadvantages	Less accuracy for complex-shape regions	Complex mesh-generator in 3D;	1. Dense matrix; 2. More complex analytics

Boundary Element Method for Stationary Problems

An integral representation for the electrostatic potential φ at observation point r is a sum of the surface sources with the density σ and space charge density ρ :

$$\varphi(\vec{r}) = \frac{1}{4\pi\varepsilon}\int_S \frac{\sigma(\vec{r}\,')}{R}dS + \frac{1}{4\pi\varepsilon}\int_V \frac{\rho(\vec{r}\,'')}{R}dV\,, \vec{r}\,' \in S, \vec{r}\,'' \in V\,, R = \left|\vec{r} - \vec{r}\,'\right|.$$

Applying the Dirichlet, Neumann conditions and continuity of electric induction at the boundary gives a set of integral equations for unknown function σ

$$\varphi(\vec{r})\ \Big|_{S1} = U_0, \quad -\frac{\partial\varphi}{\partial\vec{n}}\ \Big|_{S2} = E_0, \quad \varepsilon_+ \frac{\partial\varphi}{\partial\vec{n}}\ \Big|_{S+} = \varepsilon_- \frac{\partial\varphi}{\partial\vec{n}}\ \Big|_{S-}$$

Linear System after discretization

$$GX = F, G_{ij} = \frac{1}{h_\tau h_\eta}\sum_{m=1}^{4}\iint \frac{\psi_m(\tau,\eta)}{\left|\vec{r} - \vec{r}\,'(\tau,\eta)\right|}J(\tau,\eta)d\tau\ \ d\eta.$$

Parametric representation of the boundary

$$S = \bigcup_{k=1}^{N} S_k, x = x_k(\tau,\eta), y = y_k(\tau,\eta), z = z_k(\tau,\eta), dS = J_k(\tau,\eta)d\tau d\eta,$$

Polynomial approximation for surface sources

$$\sigma(\tau,\eta) =$$
$$\left\{\left[\sigma_{ij}(\tau-\tau_{i-1})+\sigma_{i-1,j}(\tau_i-\tau)\right](\eta-\eta_{j-1})+\left[\sigma_{i,j-1}(\tau-\tau_{i-1})+\sigma_{i-1,j-1}(\tau_i-\tau)\right](\eta_j-\eta)\right\} / h_\tau h_\eta ,$$

Linear system G σ = F with matrix elements

$$G_{ij} = \frac{1}{h_\tau h_\eta}\sum_{m=1}^{4}\iint \frac{\psi_m(\tau,\eta)}{\left|\vec{r}-\vec{r}'(\tau,\eta)\right|} J(\tau,\eta)d\tau \quad d\eta.$$

Multi-flow Gun for Klystron

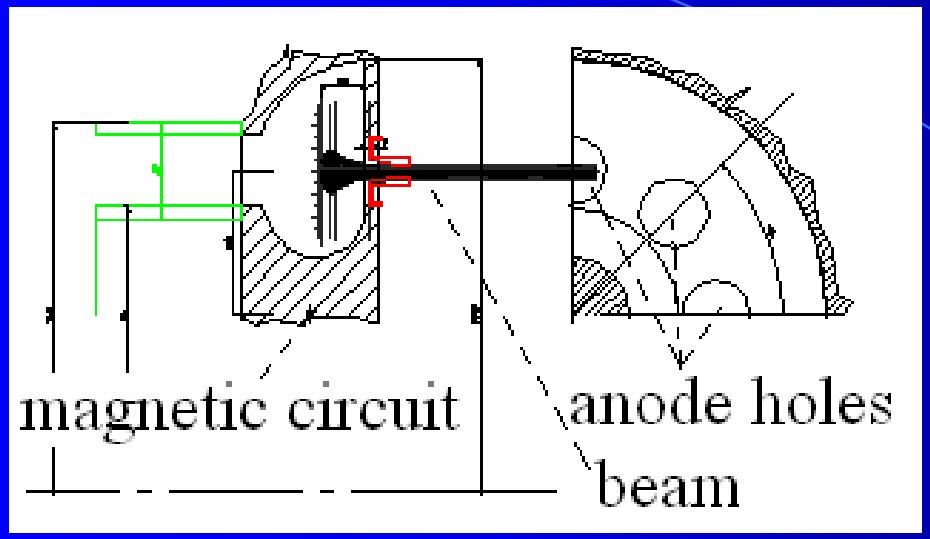

Gun schematic sketch

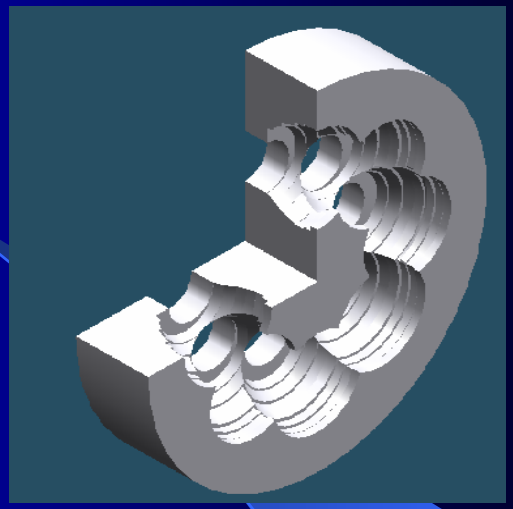

Iron geometry

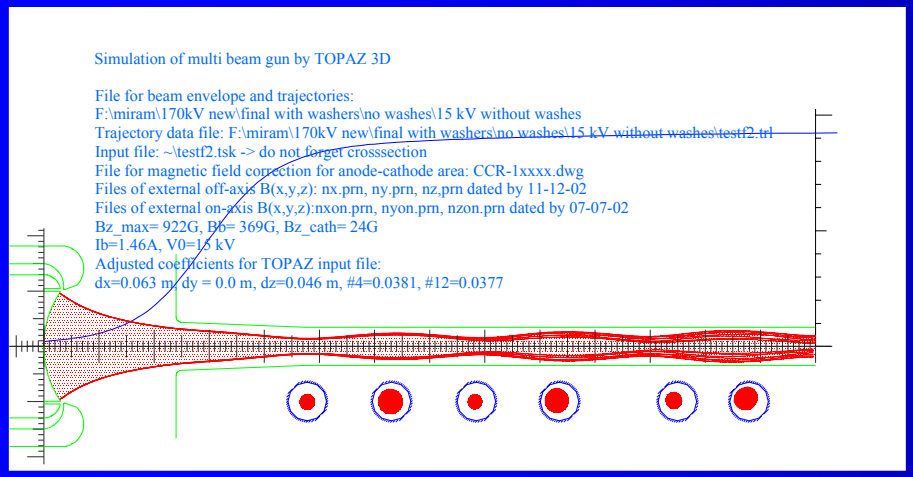

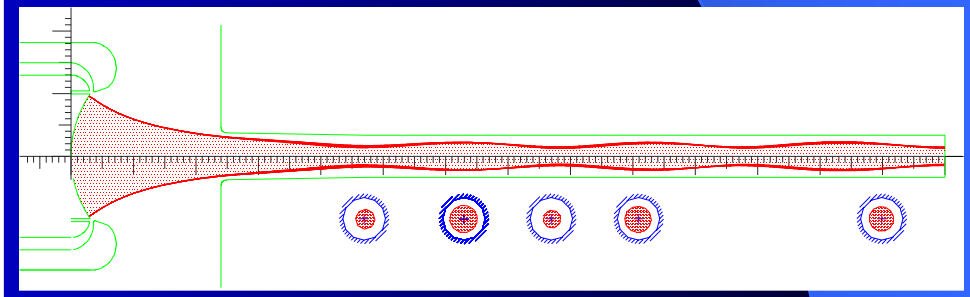

Original & optimized beam envelopes

The results of sheet-beam gun simulation

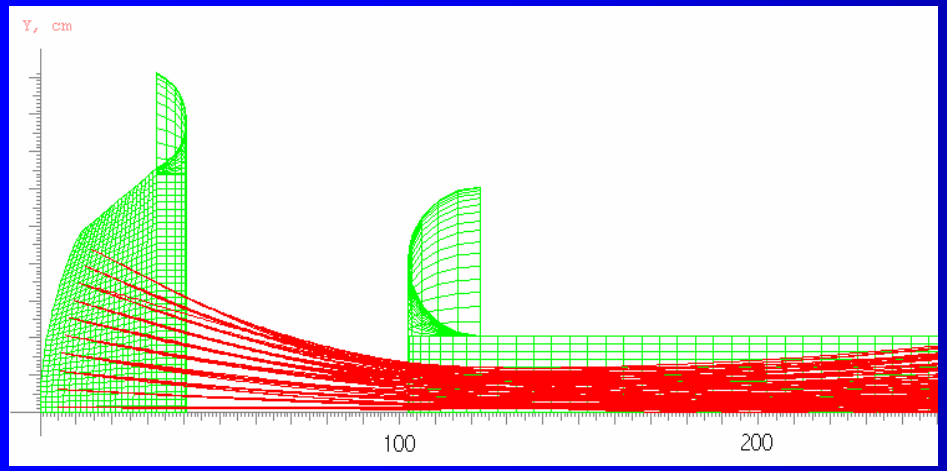

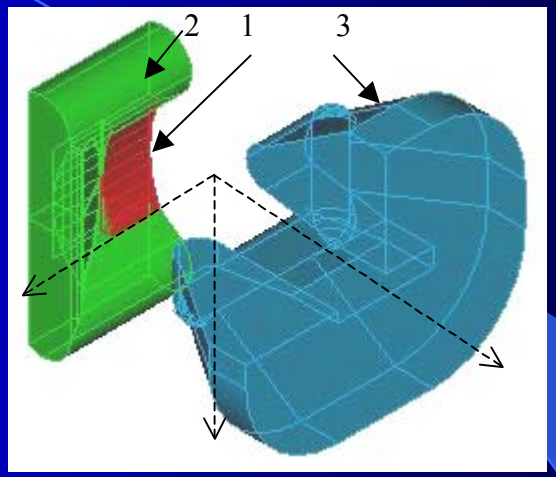

1. Focusing electrode
2. Emitter
3. Anode

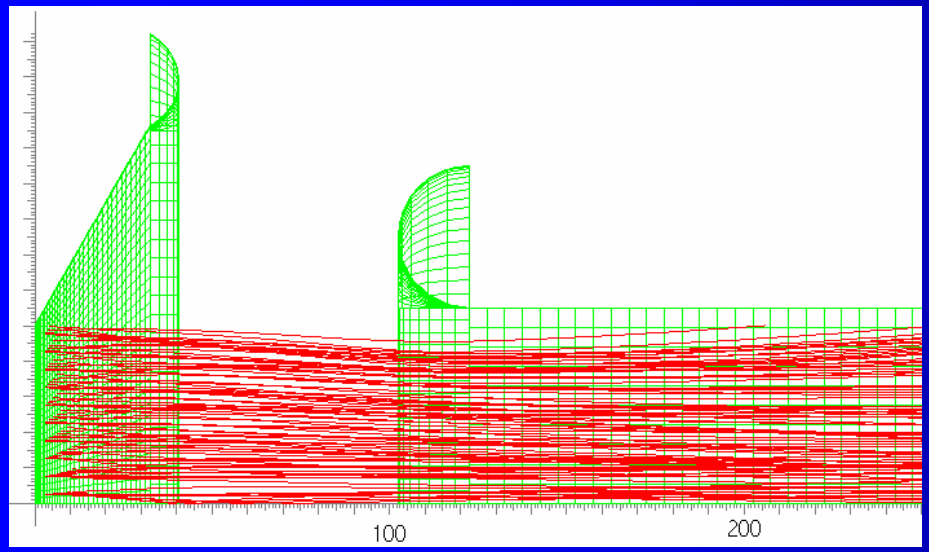

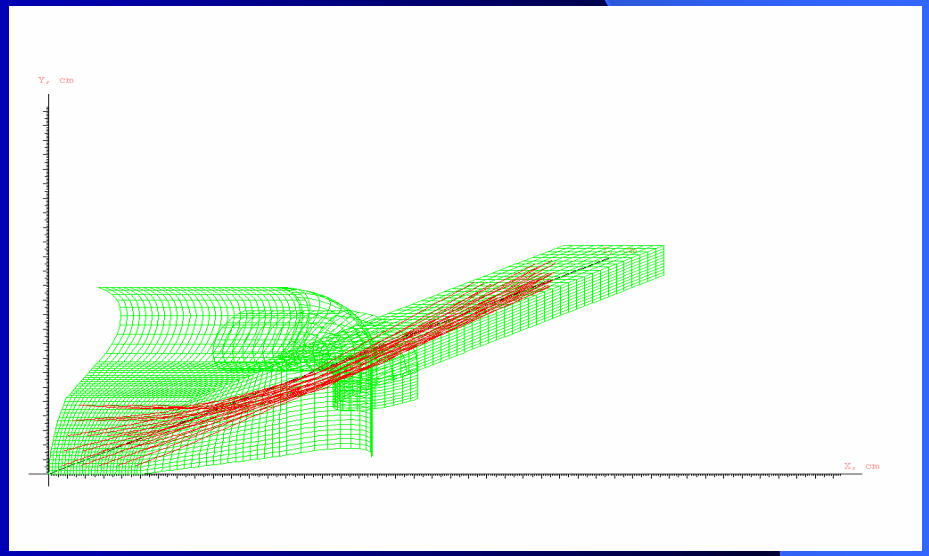

Diode, triode & grid guns

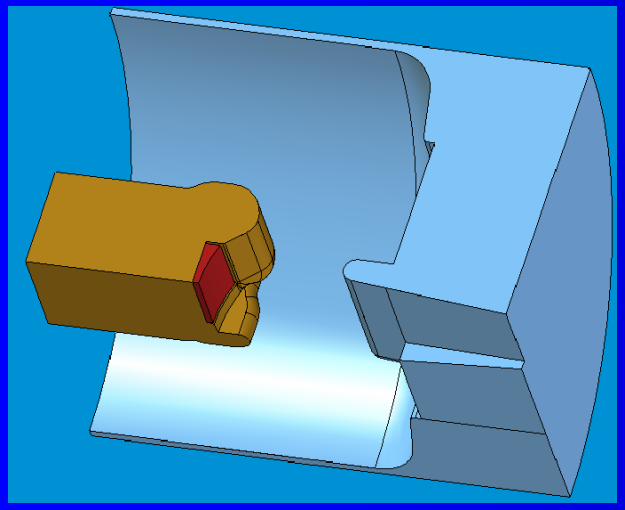

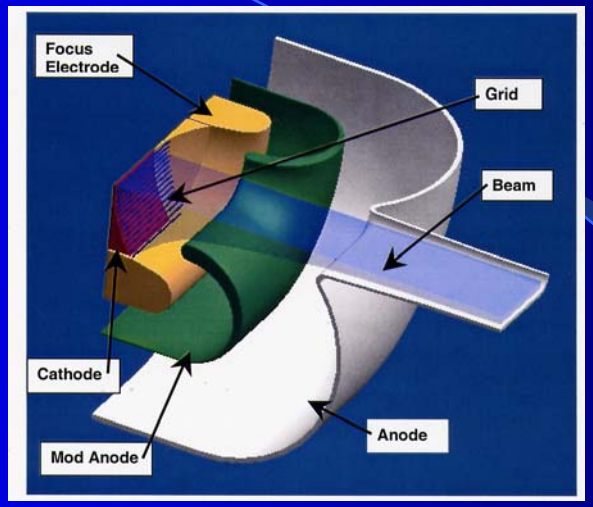

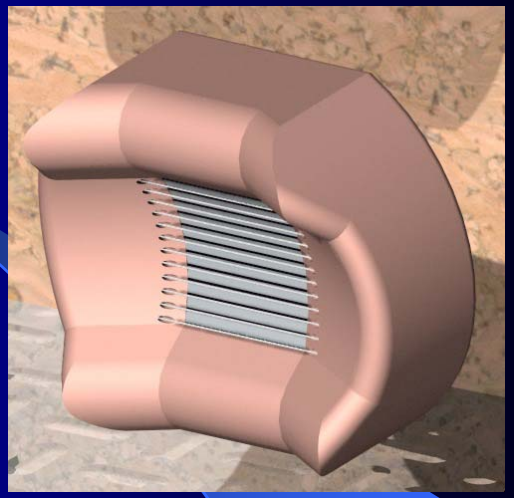

Cathode Assembly

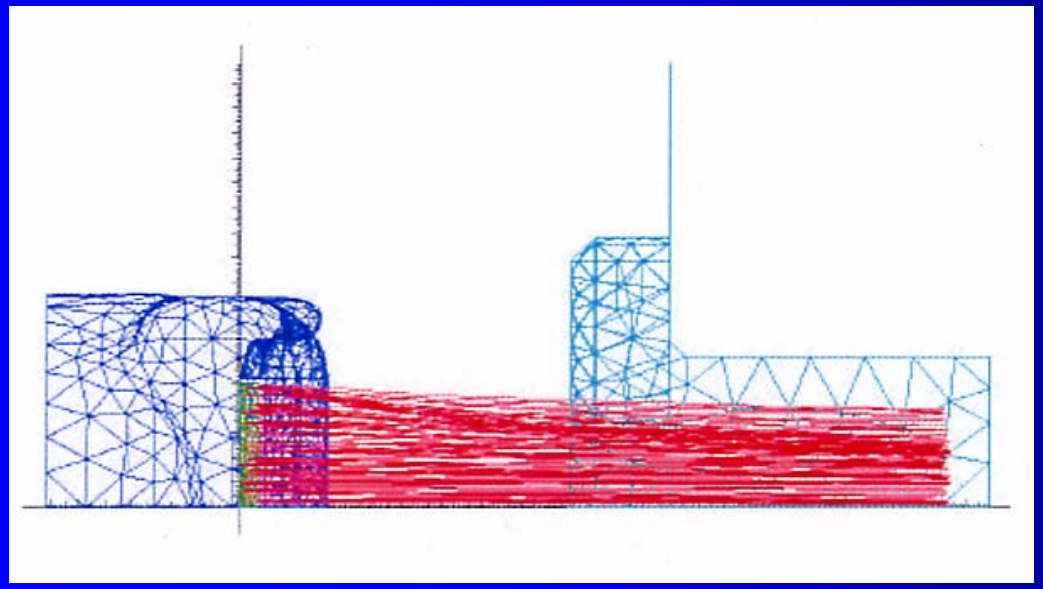

Computational Models

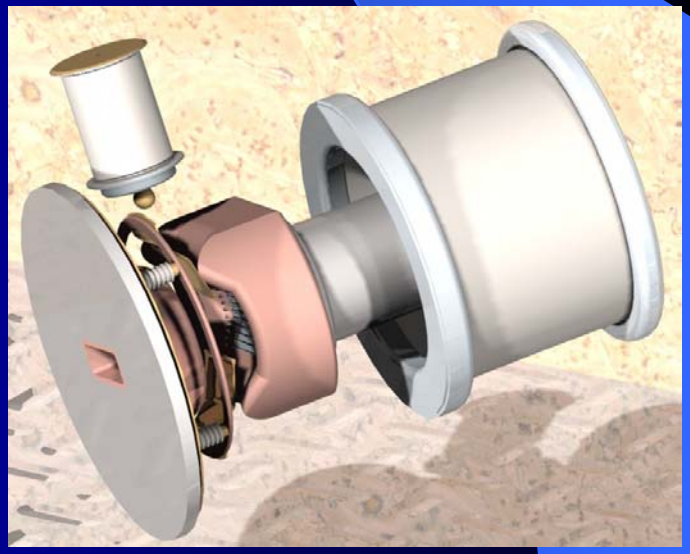

Gun Prototype, Calabazas Creek, Inc.

Non Elastic Collisions in Gas Filled Diode

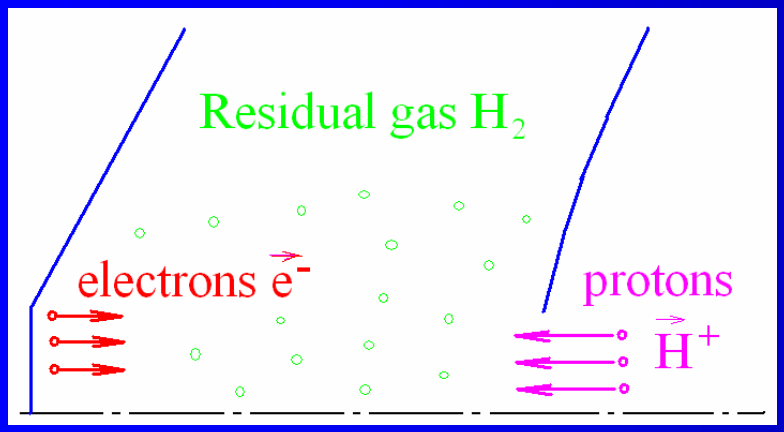

2D model of collisions

Name of reaction	Scheme
Hydrogen ionization by electrons	$\vec{e}+H_2=\vec{e}+H_2^+$
Recharging of H_2^+ on Hydrogen	$\vec{H}_2^+ + H_2 = \vec{H}_2 + H_2^+$
Dissociation of H_2^+ in Hydrogen	$\vec{H}_2^+ = \vec{H}^+ + \vec{H}$
Recharging of H^+ on Hydrogen	$\vec{H}^+ + H_2 = \vec{H} + H_2^+$
Hydrogen ionization by ions H_2^+	$\vec{H}_2^+ + H_2 = \vec{H}_2^+ + H_2^+$
Hydrogen ionization by protons	$\vec{H}^+ + H_2 = \vec{H}^+ + H_2^+$
Ionization by Hydrogen atoms H	$\vec{H} + H_2 = \vec{H} + H_2^+$
Ionization by Hydrogen molecules	$\vec{H}_2 + H_2 = \vec{H}_2 + H_2^+$
Roughing of Hydrogen atoms	$\vec{H} + H_2 = \vec{H}^+ + H_2$
Roughing of Hydrogen molecules	$\vec{H}_2 + H_2 = \vec{H}_2^+ + H_2$

$$\alpha = \sqrt{M_i / M_e}\, d n_0 \sigma_i^*$$

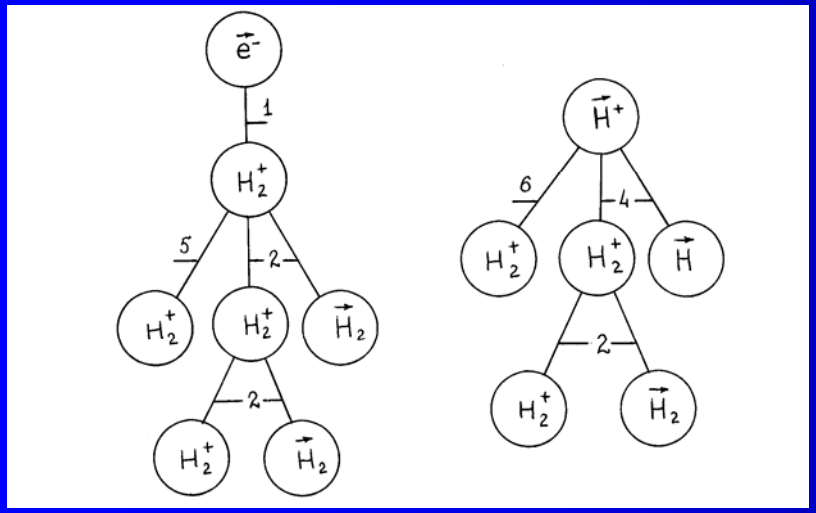

Reaction trees

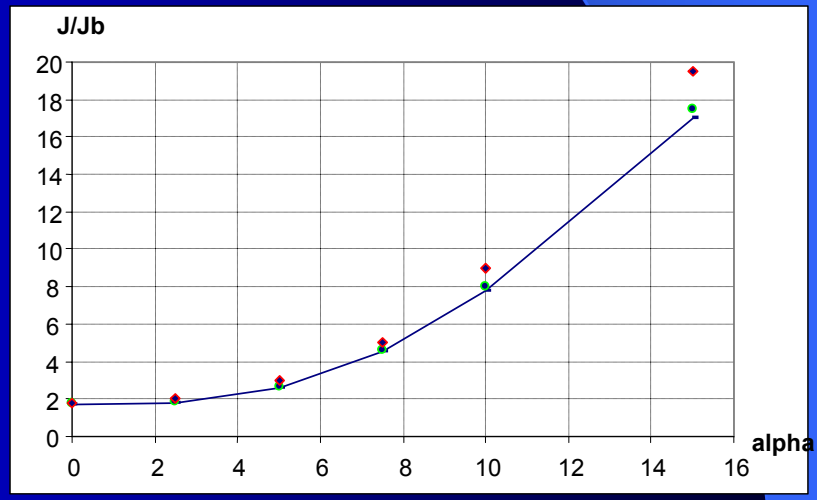

Current multiplication. Blue – 1D model, green – ionization; red – ionization+recharging

Frequency-domain Electrodynamics

Maxwell equations

$$rotE_0 = -i\omega B_0, \;\; rotH_0 = i\omega D_0 + J_0,$$

Integral representation

$$E(P) = \frac{1}{2\pi}\int_S \left[J_\beta(Q) G^e_{\alpha\beta}(P,Q) \right]_n dS_Q,$$

$$H(P) = -\frac{1}{2\pi}\int_S \left[J_\beta(Q) G^m_{\alpha\beta}(P,Q) \right]_n dS_Q.$$

Green functions

$$G^e_{\alpha\beta} = \left[\alpha \nabla \phi\right]\beta, \;\; \phi = \cos(kR)/R,$$

$$G^m_{\alpha\beta} = (\alpha\beta)\left(k\phi + \frac{1}{kR}\frac{\partial\phi}{\partial R} \right) + \frac{(\alpha R)(\beta R)}{kR^2}\left(\frac{\partial^2\phi}{\partial R^2} - \frac{1}{R}\frac{\partial\phi}{\partial R} \right)$$

Integral equations

$$H_\tau(P) = \frac{1}{\Omega - 4\pi}\int_S \left[H_\tau(Q) G^m_{\tau\eta}(P,Q) - H_\eta(Q) G^m_{\tau\tau}(P,Q) \right] dS_Q,$$

$$H_\eta(P) = \frac{1}{\Omega - 4\pi}\int_S \left[H_\tau(Q) G^m_{\eta\eta}(P,Q) - H_\eta(Q) G^m_{\eta\tau}(P,Q) \right] dS_Q.$$

Eigen modes of RF cavities

The codes MAXWELL-2 and MAXWELL-3 can simulate azimuthally harmonics and 3D modes of oscillations

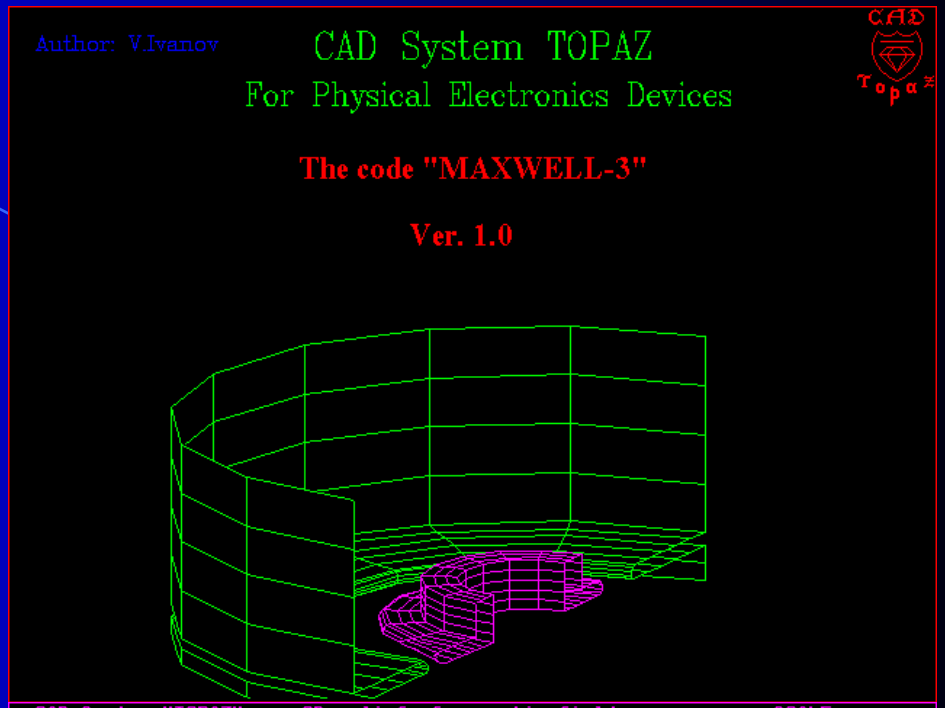

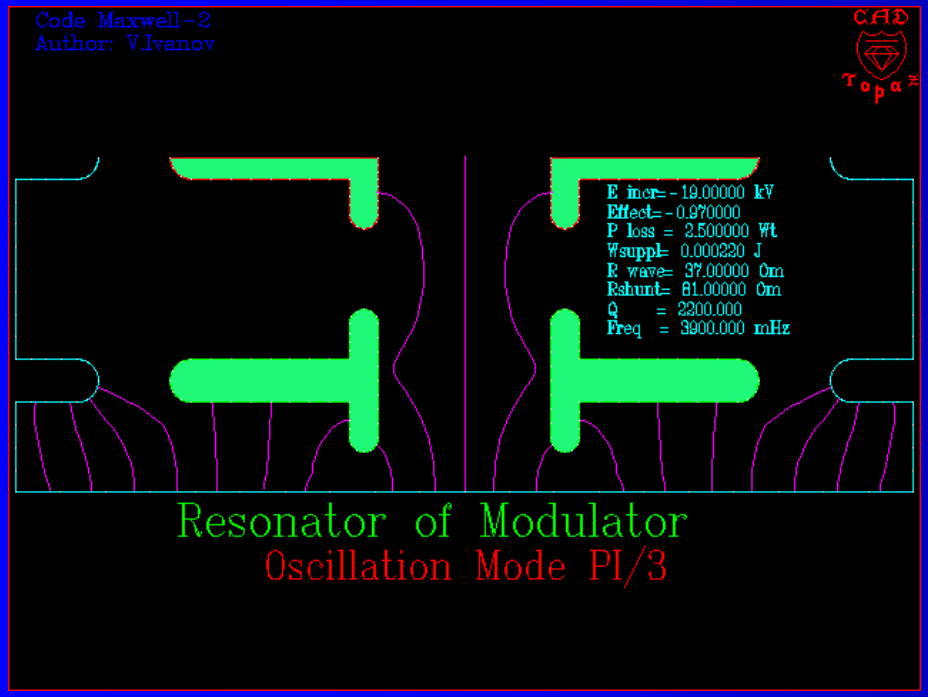

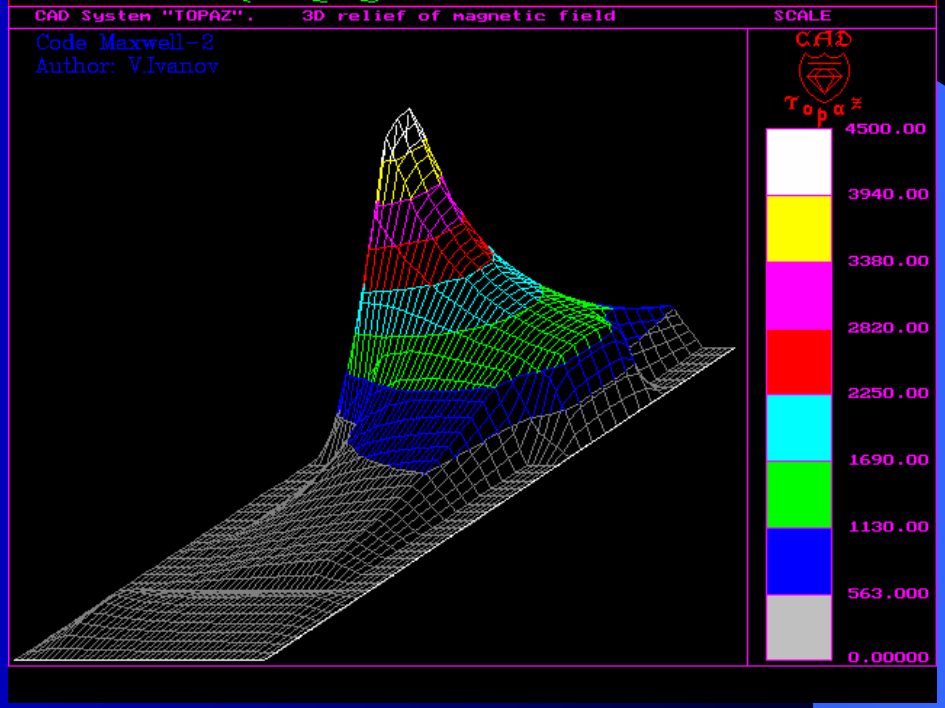

Time-domain Electrodynamics

Maxwell equations

$$\frac{\partial B^k}{\partial t} + \frac{\varepsilon^{k\alpha\beta}}{\sqrt{g}} \nabla_\alpha E_\beta = 0,$$

$$\frac{\partial D^k}{\partial t} - \frac{\varepsilon^{k\alpha\beta}}{\sqrt{g}} \nabla_\alpha H_\beta = J^k.$$

Material equations

$$J^i = \sigma E^i + J_0^i(t,r), \;\; B^i = \mu_{ik}(H) H^k, \;\; D^i = \varepsilon_{ik}(E) E^k.$$

Conservation law

$$\frac{\partial \rho}{\partial t} + div\ J_c = 0.$$

RF-gun design for LCLS. The code MAXWELL-T

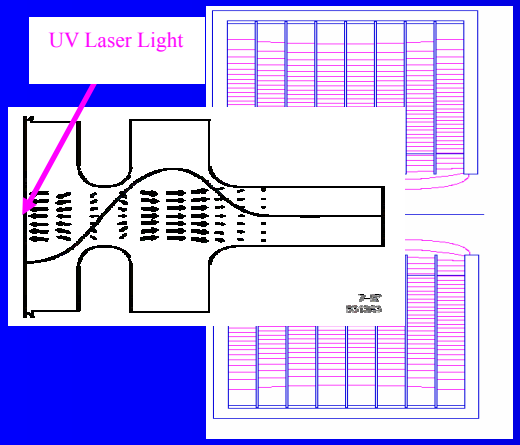

RF Photoinjector

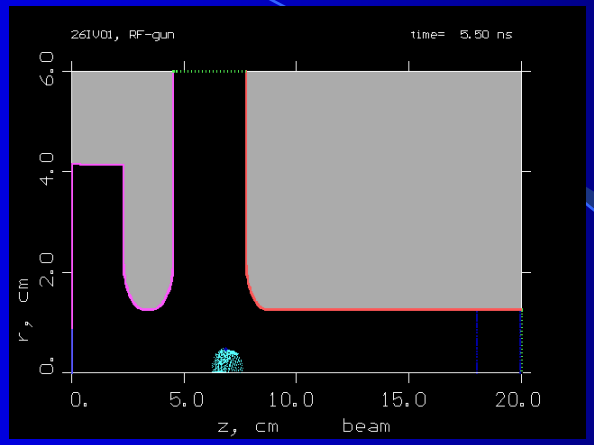

10 ps, 1 nQ bunch dynamics

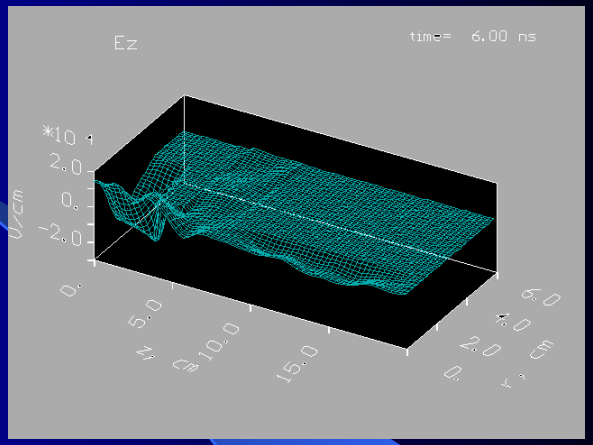

Electric field distribution

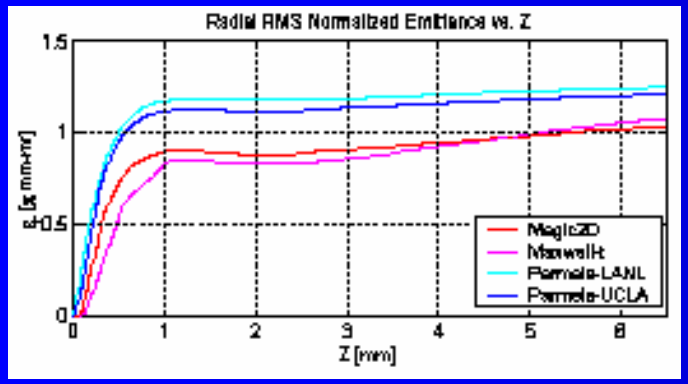

Transverse normalized emittance vs. z

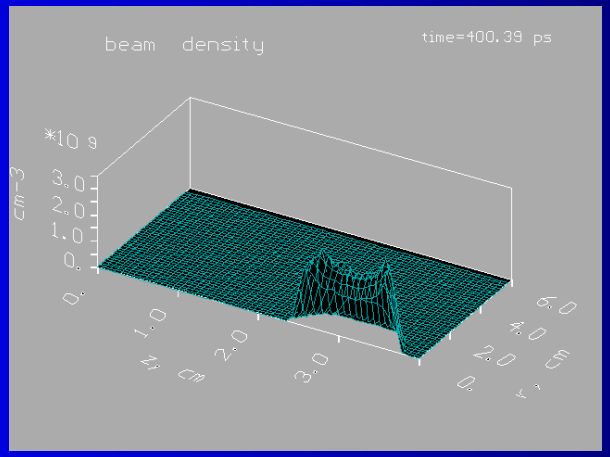

Space charge distribution

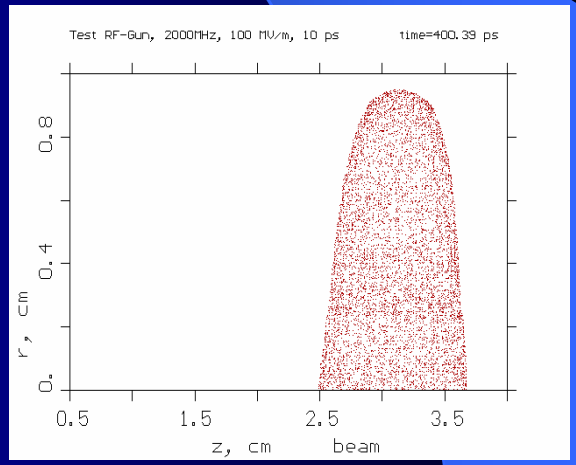

Space charge profile

Transverse charge distribution

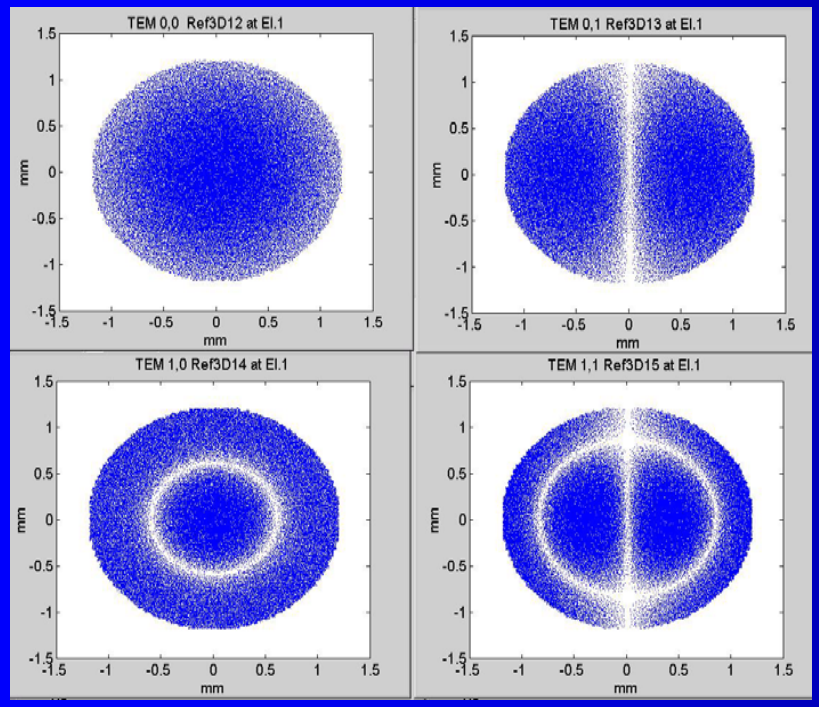

At the cathode

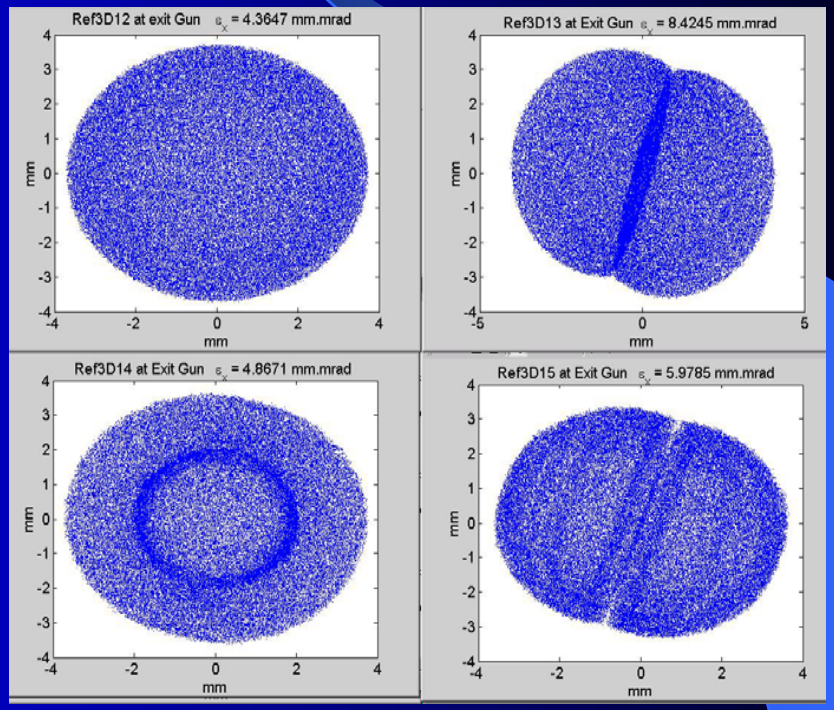

At the exit

Beam Optics

Klystron gun design using different numerical methods

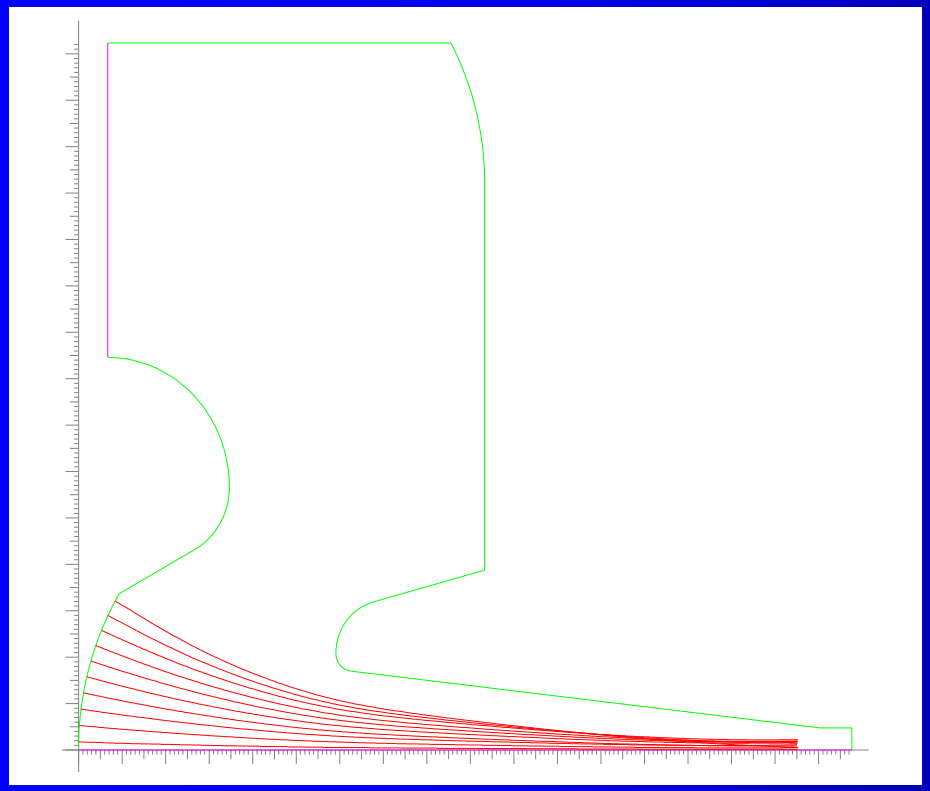

Stationary problem. BEM.

The code “POISSON-2”. T=5”

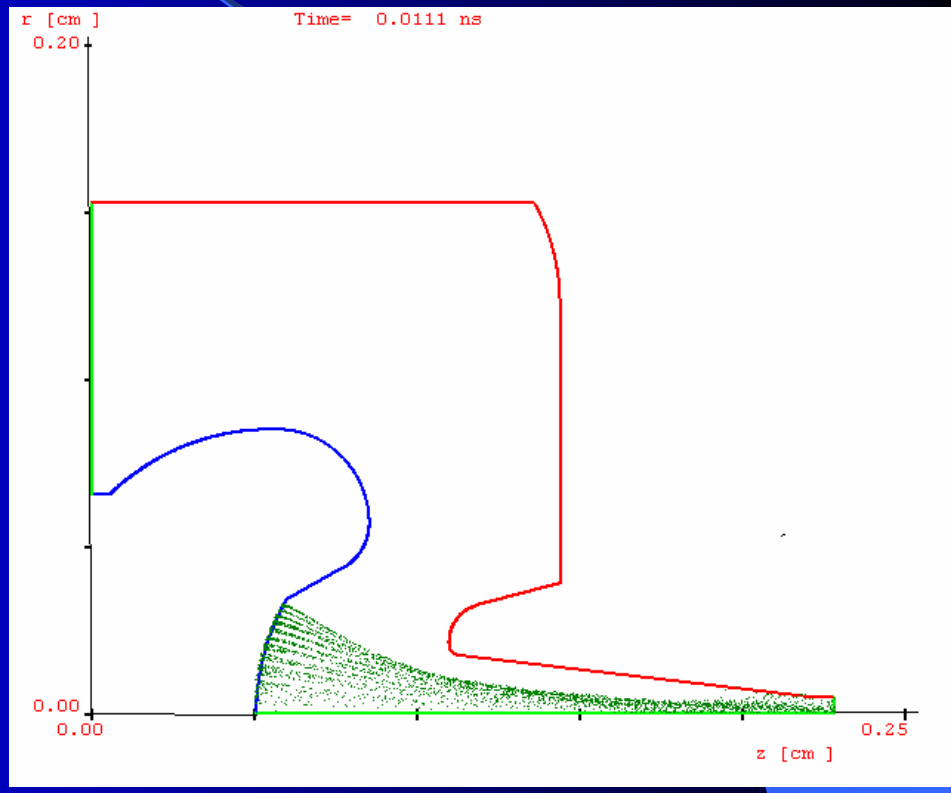

Non Stationary problem. FDM + PIC.
The code “MAXWELL-T”,
Mesh: 400x500. Np=3500, T= 65”

Time-of-flight Mass-Spectrometer

Portable high resolution TOF MS for analysis of Green-house gases

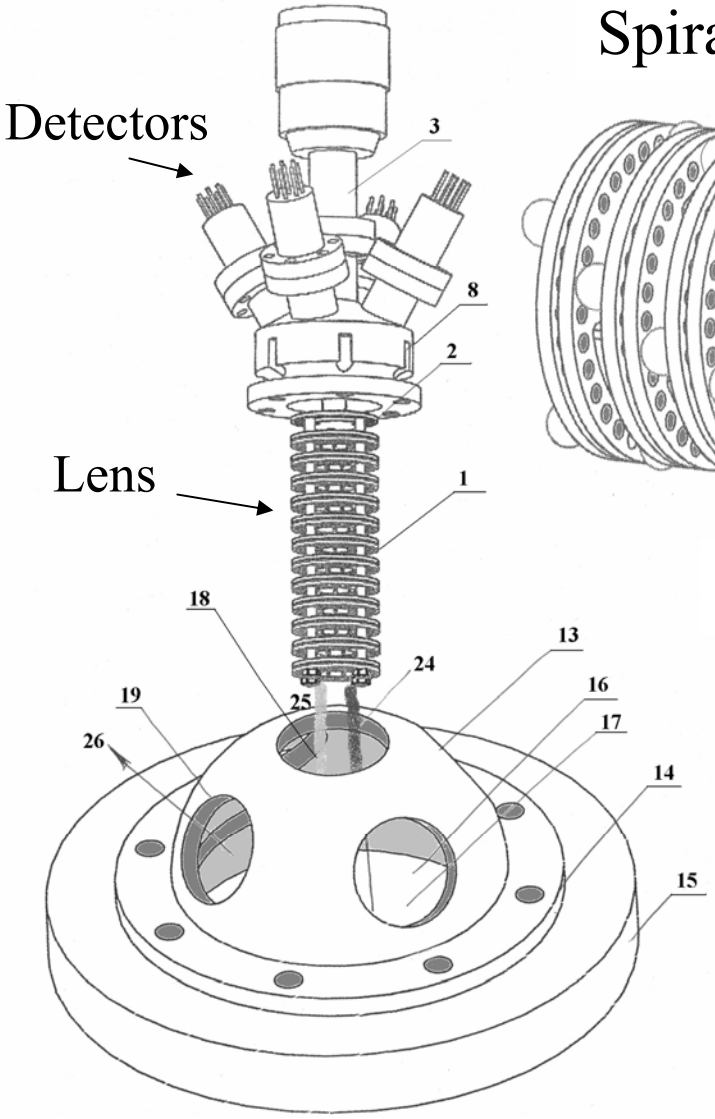

Spiral-Quadruple Lens

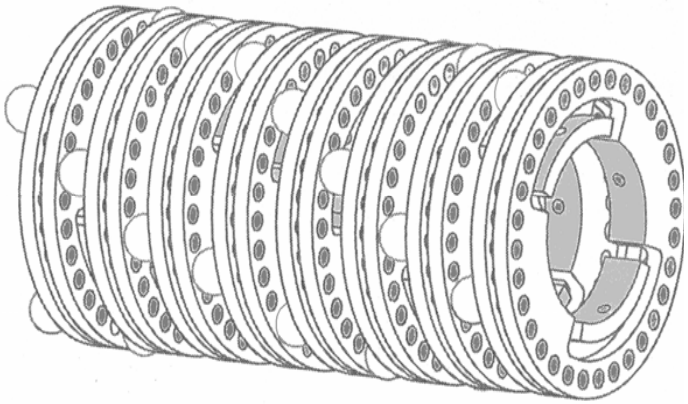

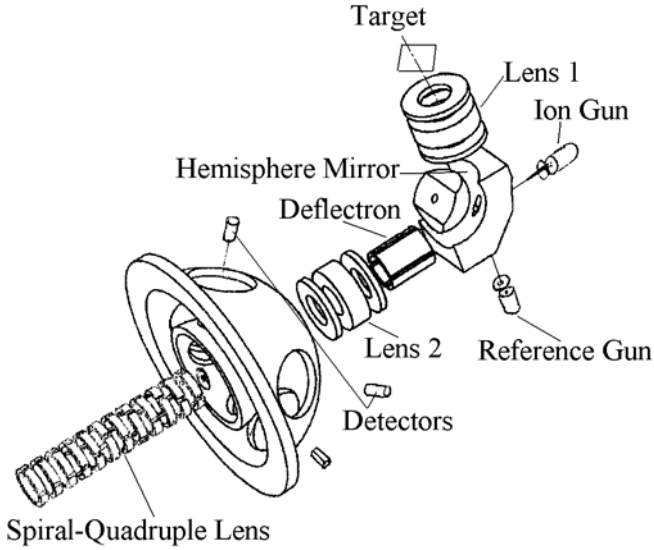

Temporal Resolution for Green-house gases

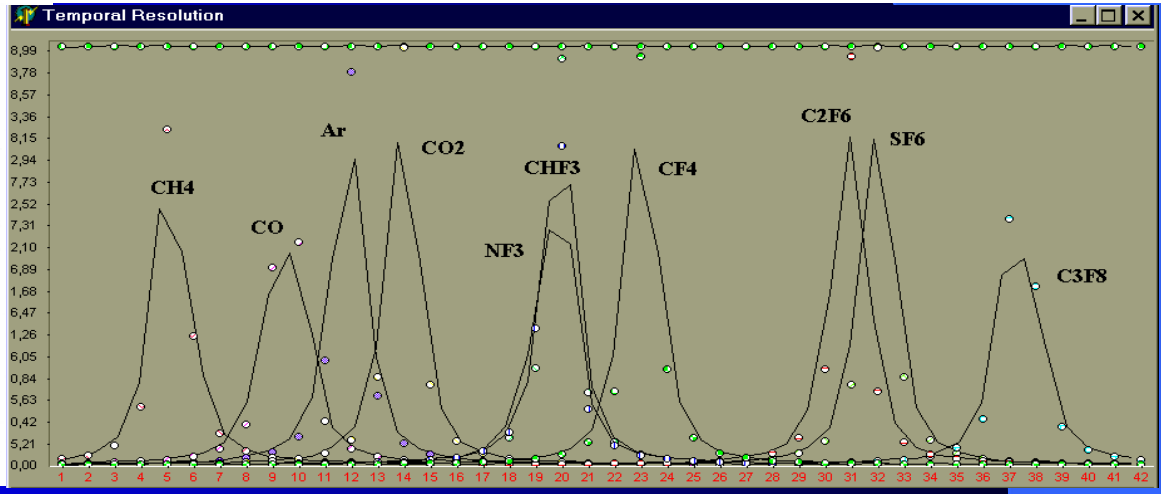

Dark Current simulation model

Field emission

$$J_f(r,t) = 1.54\times10^{\left(-6+\frac{4.52}{\sqrt{\varphi}}\right)} \frac{(\beta E)^2}{\varphi} e^{\left(\frac{-6.53\times10^9 \varphi^{1.5}}{\beta E}\right)},$$

Secondary emission

σ = Isec / Ipri = δ + η+ r

$$\delta = \frac{\delta_m}{g_m} g\left(z_m \frac{\varepsilon}{\varepsilon_m}\right), \quad g(z) = z^{-n}\left[1 - e^{-z^{n+1}}\right],$$

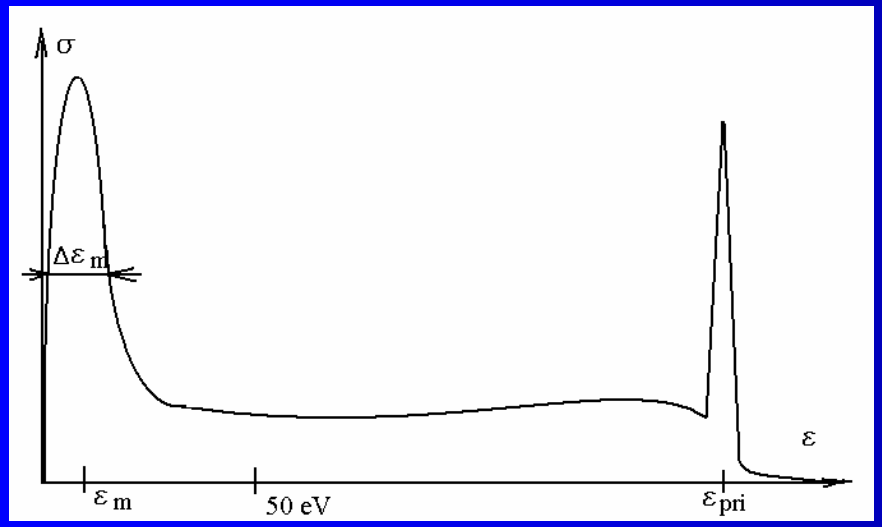

Secondary emission spectrum

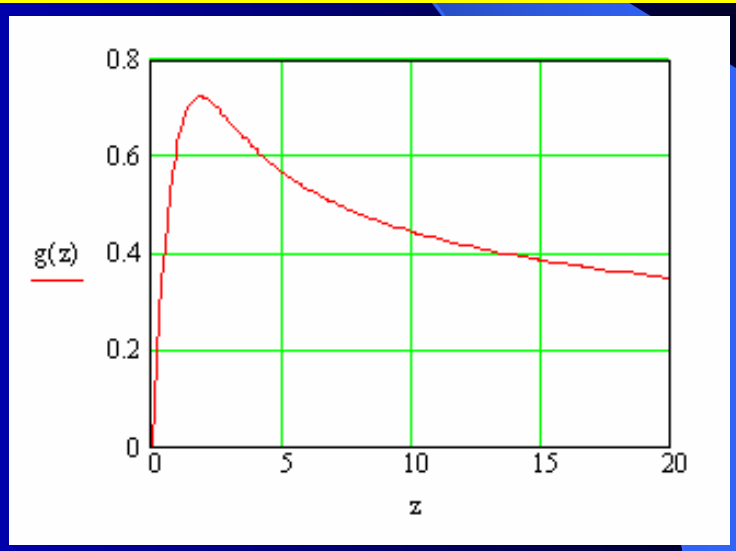

Lye-Dekker model

SLAC X-band TW-structure

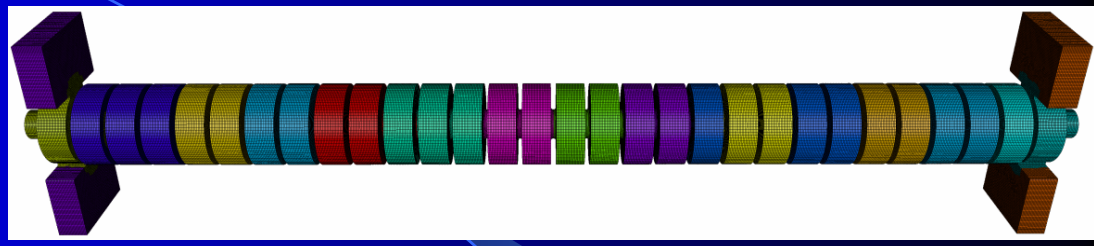

30-cell structure,
11.424GHz, G=62MV/m

Distributed mesh for parellell
Mawxell solver

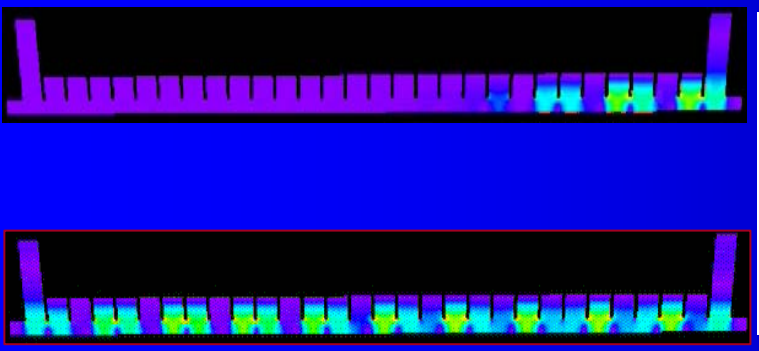

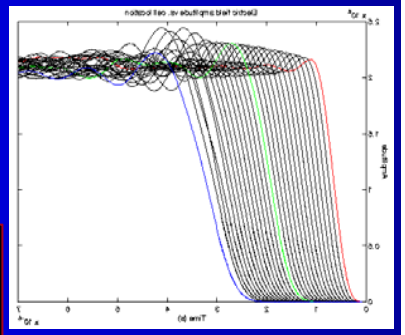

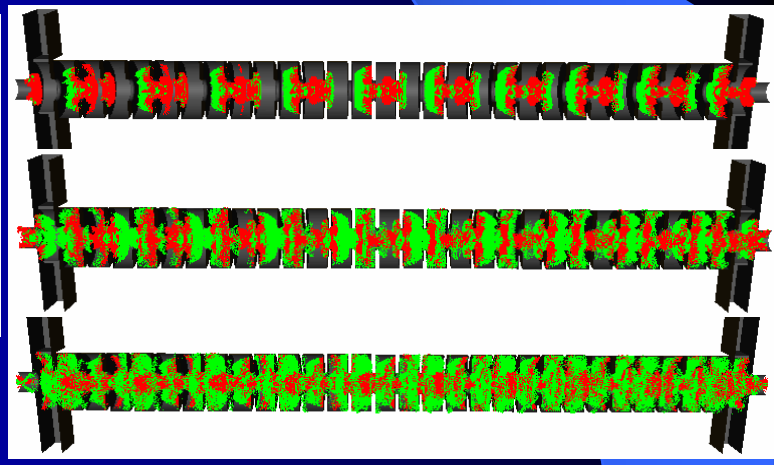

Transient EM-field. Electric field
overshoot for rise-time 15 ns

Dark current evolution. Red-
primary part., green –secondaries

NLC Dark Current Pulse

Dark current pulses were obtained for the ***FIRST TIME*** from **Track3P** simulation for direct comparison with measurement

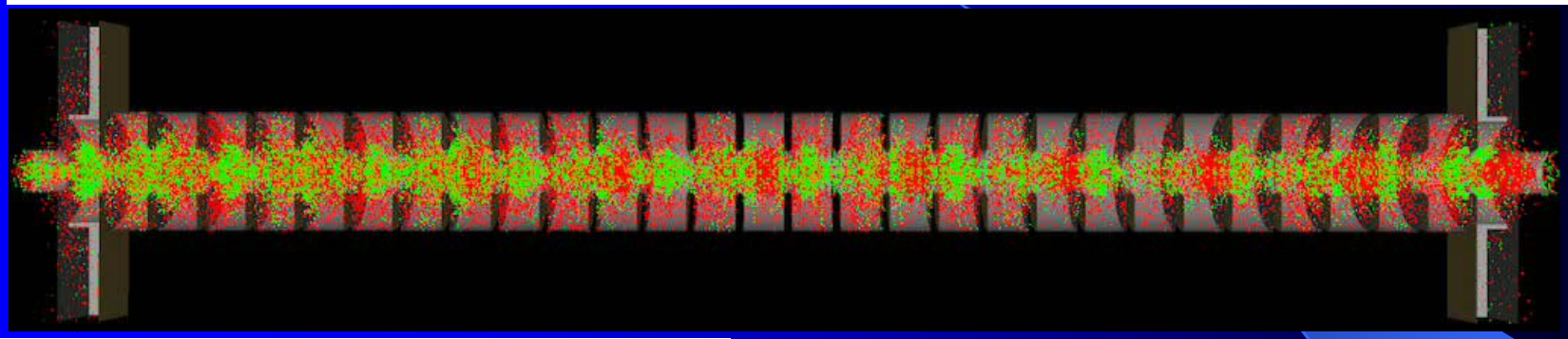

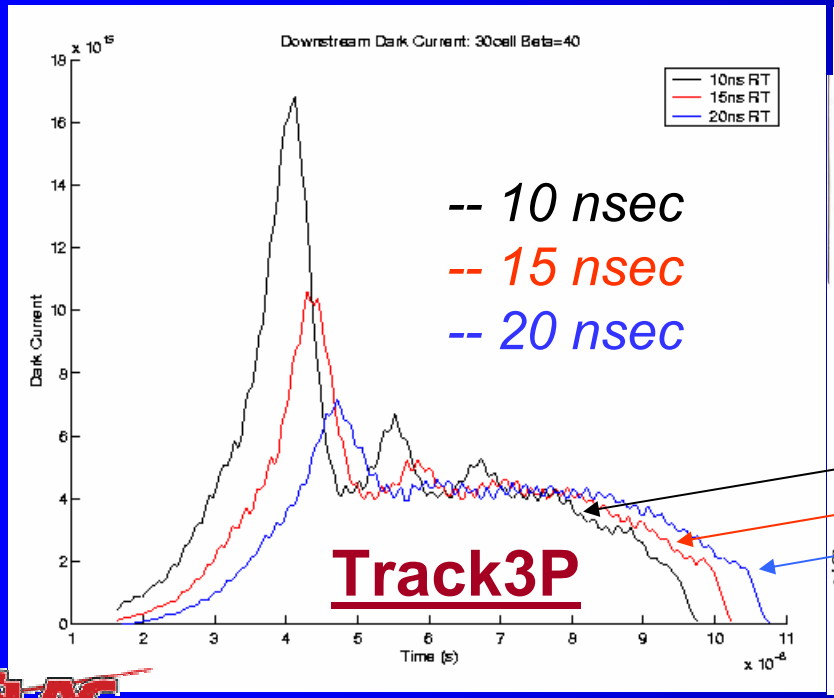

Dark current @ 3 pulse risetimes

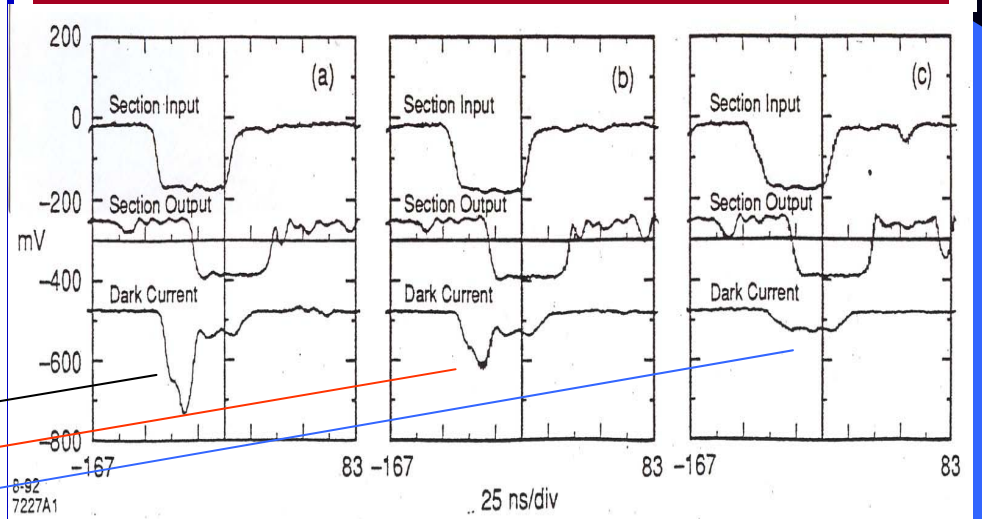

of the RF pulse for 30-cavity TW section tests.

Experimental data by J Wang

X-Ray spectrum simulation for Square bend waveguide

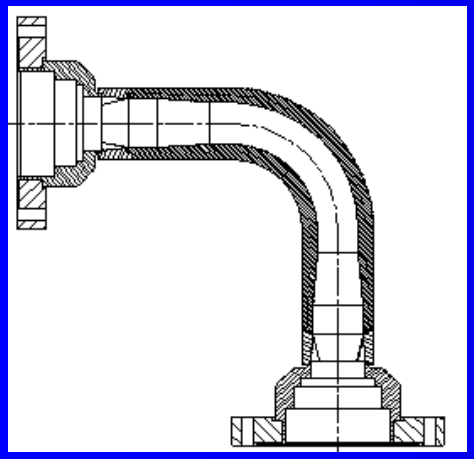

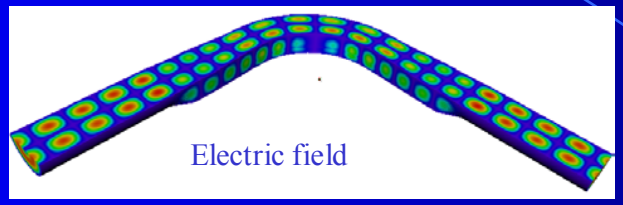

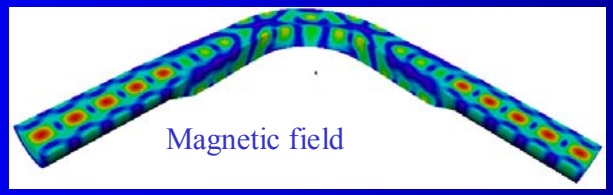

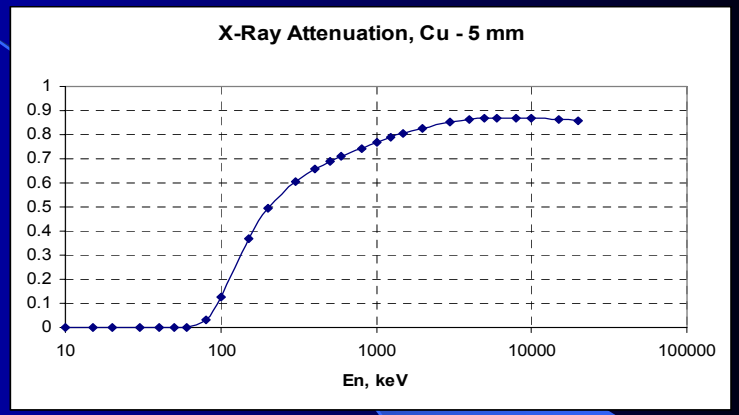

Square bend waveguide & EM fields

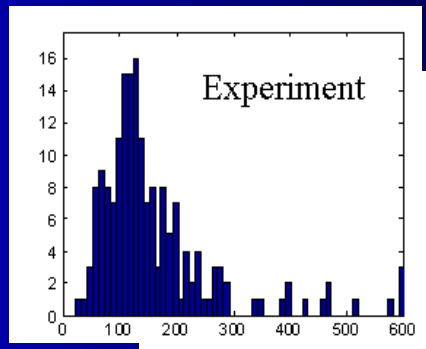

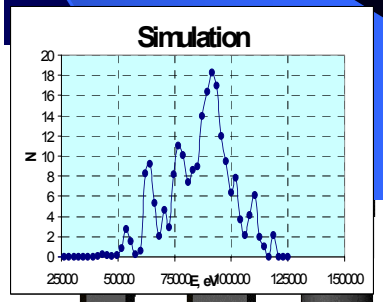

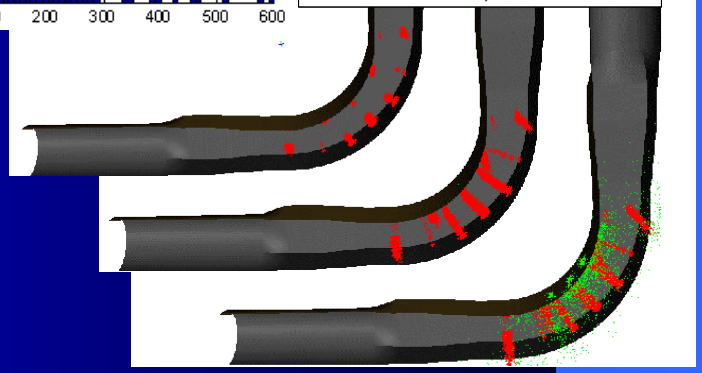

X-ray energy spectrum. Experimental data by C. Adolphsen, simulation by V. Ivanov

Multipactoring in super conducting cavity

Multipactoring effect is the main factor limiting field gradient in SC cavities

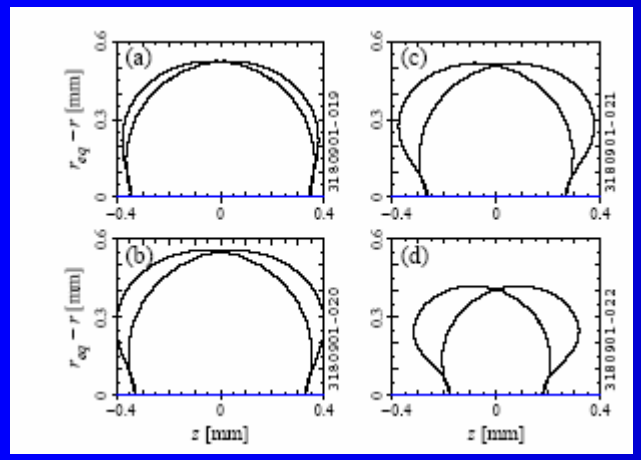

MultiPac simulations

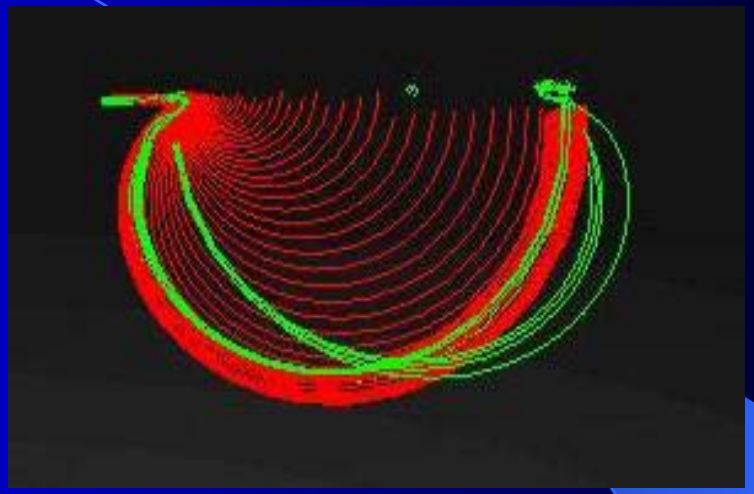

Track3P simulation

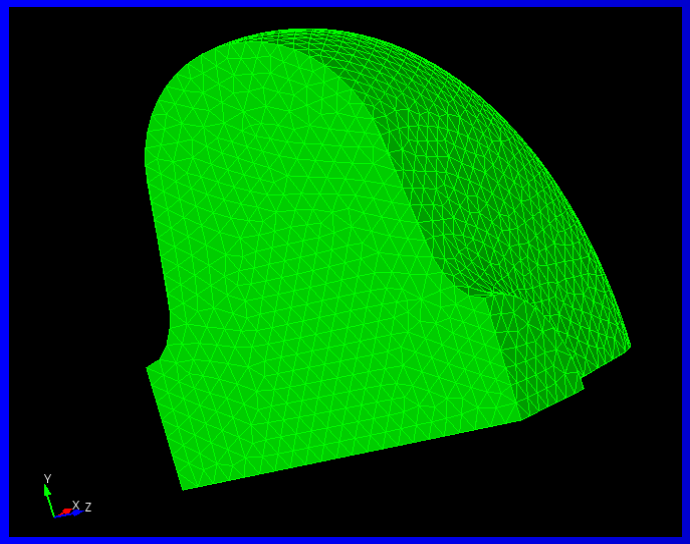

Meshing for SNS Cavity

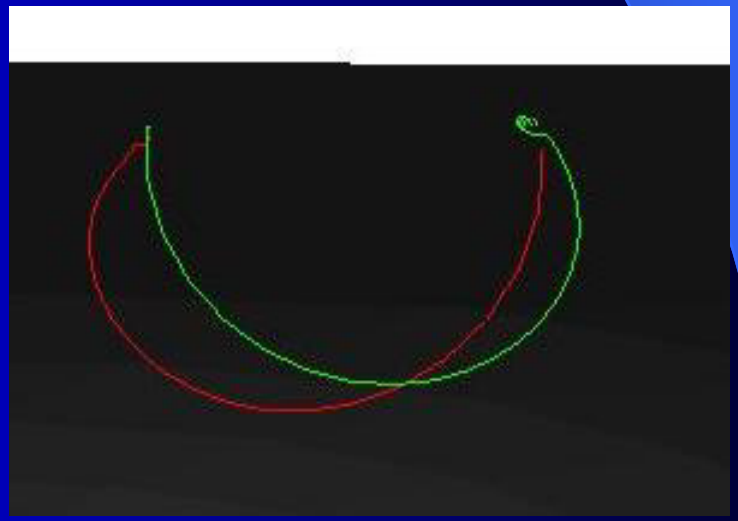

G = 59 MV/m

Aberrational approach

Trajectory equation

$$r'' + \frac{1 + r'r'^*}{\varepsilon + \varphi}\left(\frac{r}{2}\frac{\partial \varphi}{\partial z} - \frac{\partial \varphi}{\partial r^*}\right) + \sqrt{\frac{q}{2m}\frac{1 + r'r'^*}{\varepsilon + \varphi}}\left[r'\frac{\partial \psi}{\partial z} + r'^2\frac{\partial \psi}{\partial r} - (2 + r'r'^*)\frac{\partial \psi}{\partial r^*}\right] = 0, r = x + iy.$$

Field expansion

$$\varphi(r, z) = \Phi(z) - \frac{rr^*}{4}\Phi''(z) + \frac{(rr^*)^2}{64}\Phi^{IV}(z) - \cdots$$

Paraxial equation

$$u'' + \frac{\Phi'(z)u'}{\Phi(z) + \varepsilon_z} + \frac{\Phi''(z) + \rho(z)/\varepsilon_0 + \sqrt{q/2m}B_z(z)}{\Phi(z) + \varepsilon_z}u = 0, u = re^{i\xi(z)}.$$

Principal trajectories

$$\upsilon(z_0) = 0,\ \ w(z_0) = 1,\ \ \upsilon'(z_0) = 1/\sqrt{\varepsilon_z},\ \ w'(z_0) = 1/R_c.$$

Aberrational expansion

$$r = \sqrt{\varepsilon_r}\upsilon e^{i\alpha} + r_0 w e^{i\beta} + \sqrt{\varepsilon_r \varepsilon_z}He^{i\alpha} + r_0\sqrt{\varepsilon_z}Ke^{i\beta} + \varepsilon_r^{3/2}Be^{i\alpha} + \sqrt{\varepsilon_r}\varepsilon_z Pe^{i\alpha} +$$
$$r_0\varepsilon_z Qe^{i\beta} + r_0^2\sqrt{\varepsilon_r}\left[Ce^{i(2\beta-\alpha)} + De^{i\alpha}\right] + r_0\varepsilon_r\left[Fe^{i(2\alpha-\beta)} + Ge^{i\beta}\right] + r_0^3 E + \cdots.$$

High-speed streak camera

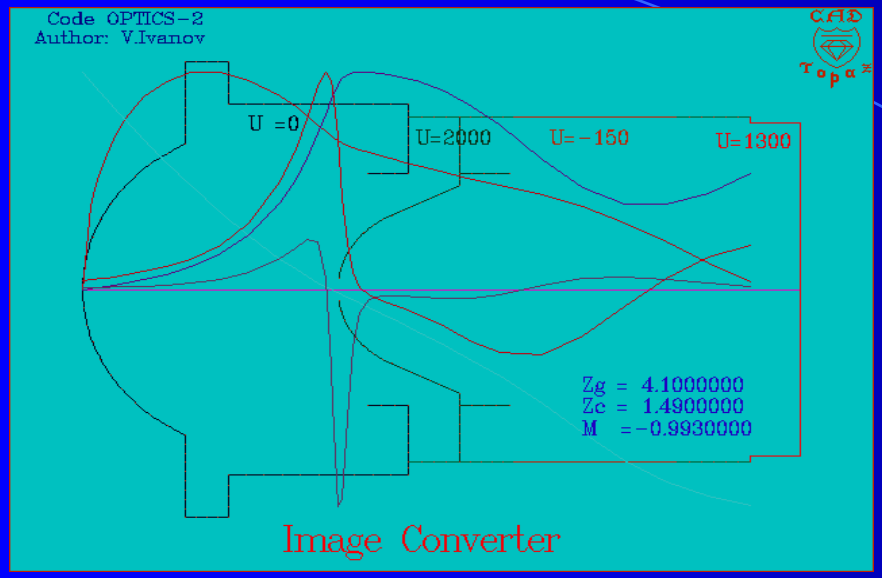

Infrared image converter

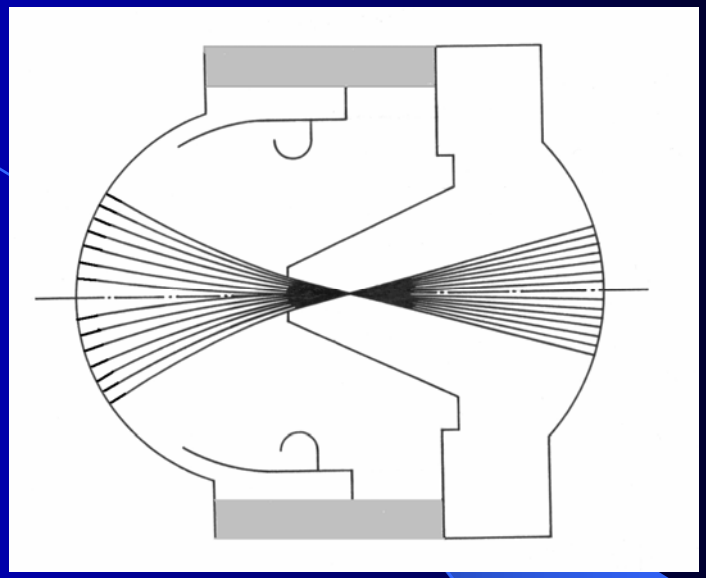

Night vision glasses

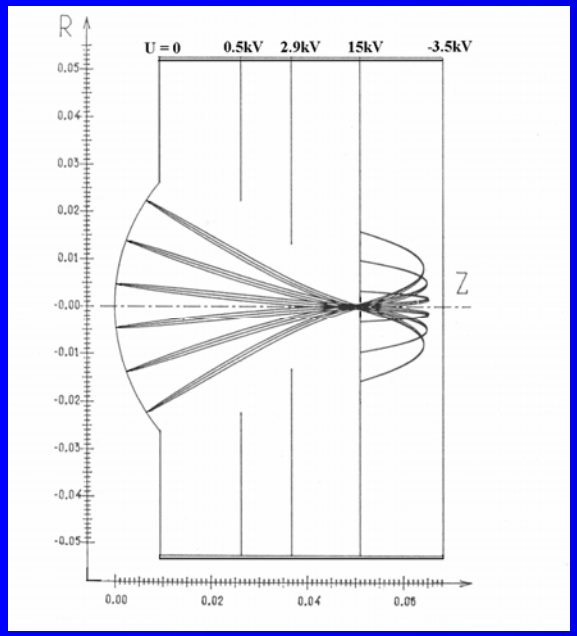

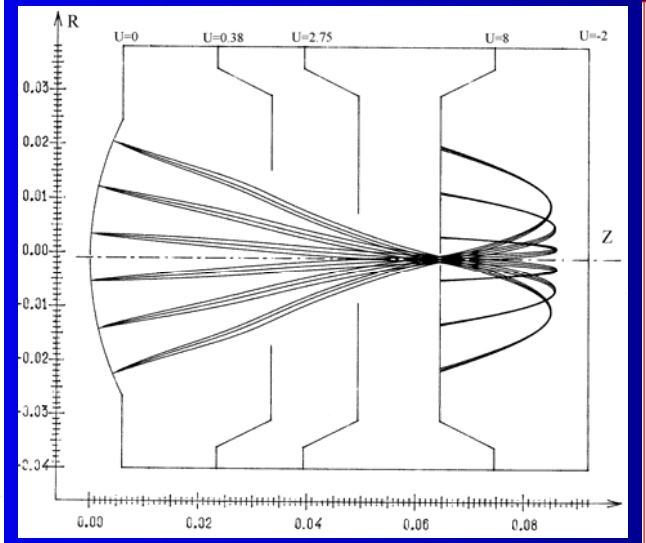

X-ray light amplifier

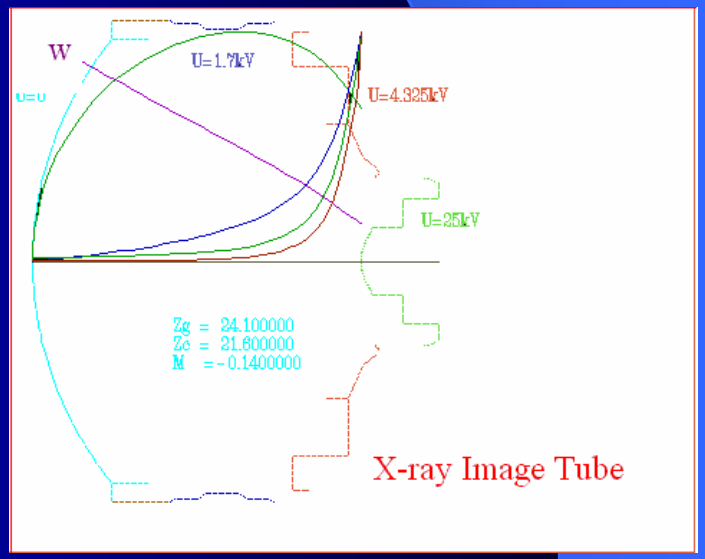

Optimization Problem

Objective functional

$$F_0\left\{\vec{r}(\vec{u}),\vec{E}(\vec{u}),\vec{H}(\vec{u})\right\} \Rightarrow \min(\vec{u} \in U)$$

Constraints

$$F_i\left\{\vec{r}(\vec{u}),\vec{E}(\vec{u}),\vec{H}(\vec{u})\right\} < 0,\ \ i = 1,n;$$

$$F_i\left\{\vec{r}(\vec{u}),\vec{E}(\vec{u}),\vec{H}(\vec{u})\right\} = 0,\ \ i = n,N;$$

Optimization domain U:

$$\overset{-}{\ }_j < \ \ _j < u_j^+,\ \ j = 1,m.$$

Original equation

$$\int_S \sigma_Q G_{PQ} dS_Q + \lambda\sigma_P = U_P.$$

Equation in variations

$$\int_S \delta\sigma_Q G_{PQ} dS_Q + \lambda\delta\sigma_P = \delta U_P - \int_S \sigma_Q \delta G_{PQ} dS_Q.$$

Types of the geometry perturbations

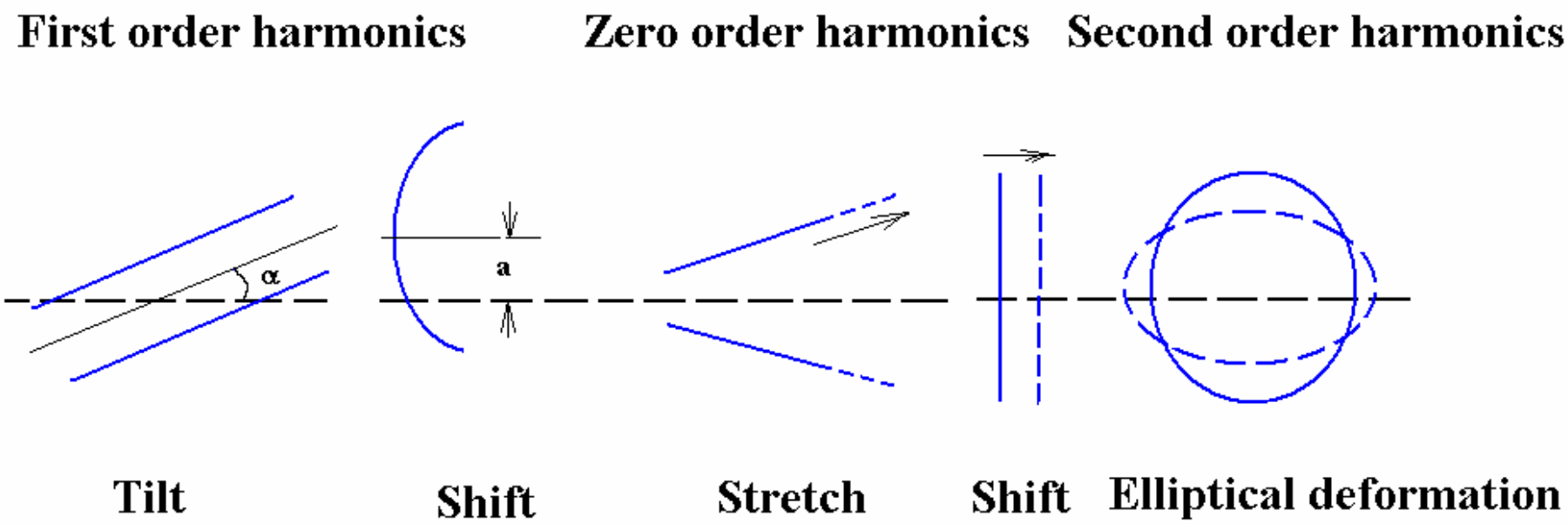

Boundary problems

Fourier expansion

$$\varphi(r,z,\theta) = \Phi(z) + \sum_m \varphi_m(r,z)\cos[m(\theta+\theta_m)]$$

Helmholtz equations

$$\frac{\partial^2\varphi_m}{\partial r^2} + \frac{\partial^2\varphi_m}{\partial z^2} + \frac{1}{r}\frac{\partial\varphi_m}{\partial r} - \frac{m^2}{r^2}\varphi_m = \rho_m$$

with the boundary conditions

$$\varphi_m\Big|_{S1} = U_m(r,z); \qquad \frac{\partial\varphi_m}{\partial\vec{n}}\Big|_{S2} = \vec{E}_m(r,z).$$

Algorithms of BEM

Integral equation

$$\int_{S1} \sigma_m(Q)\ \ G_{\sigma,m}(P,Q)dS = U_m(P) - \int_V \rho_m(t) G_{\rho,m}(P,Q)dV,$$

$$\frac{\sigma_m(P)}{2} - \int_{S2} \sigma_m(Q) G_{\sigma,m}(P,Q)dS = E_m(P) - \int_V \rho_m(t) G_{\rho,m}(P,Q)dV.$$

Kernels

$$G_{\sigma,m} = r' \int_0^{2\pi} \frac{\cos(m\theta)d\theta}{\sqrt{r^2 + (r')^2 - 2rr'\cos\theta + (z-z')^2}},$$

$$G_{\nu,m} = r' \int_0^{2\pi} \frac{[(z-z')\sin(\vec{n}\vec{e}_z) - (r - r'\cos\theta)\cos(\vec{n}\vec{e}_z)]\cos(m\theta)d\theta}{[r^2 + (r')^2 - 2rr'\cos\theta + (z-z')^2]^{3/2}}.$$

Boundary Variations for the Electron Optical Device

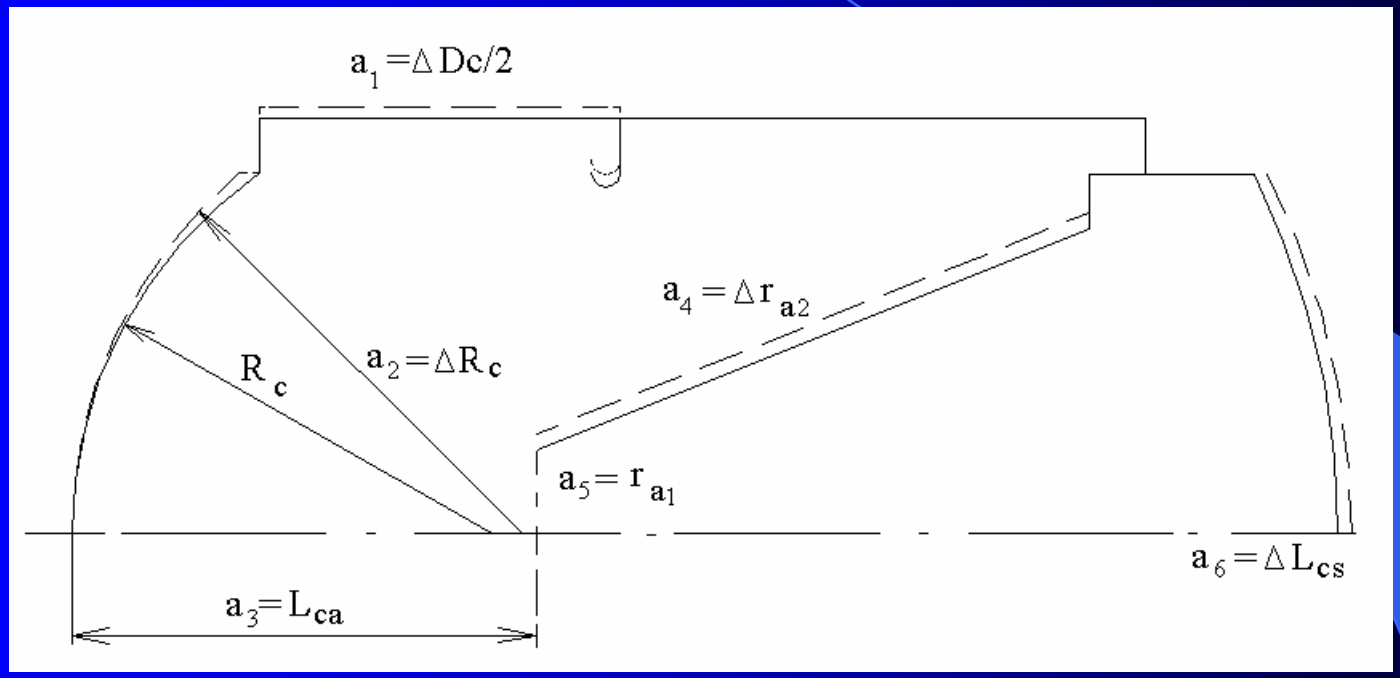

a_1 – change of the tube diameter; a_2 – change curvature radius for the cathode ; a_3 – change of the radius for the anode hole; a_4 – change of the outer radius for the anode cone; a_5 – change of the cathode-anode distance; a_6 – change of the cathode-anode distance

Non perturbed potential and derivatives

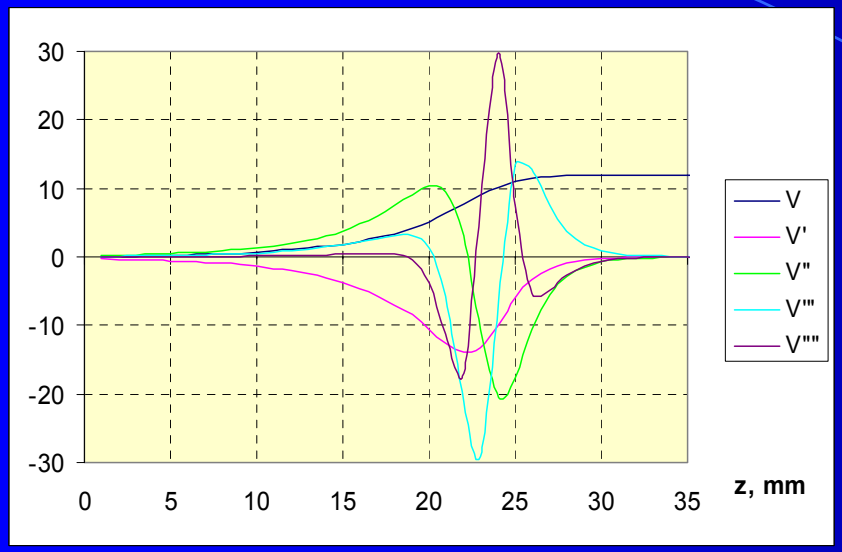

Variation of the cathode radius (m=1)

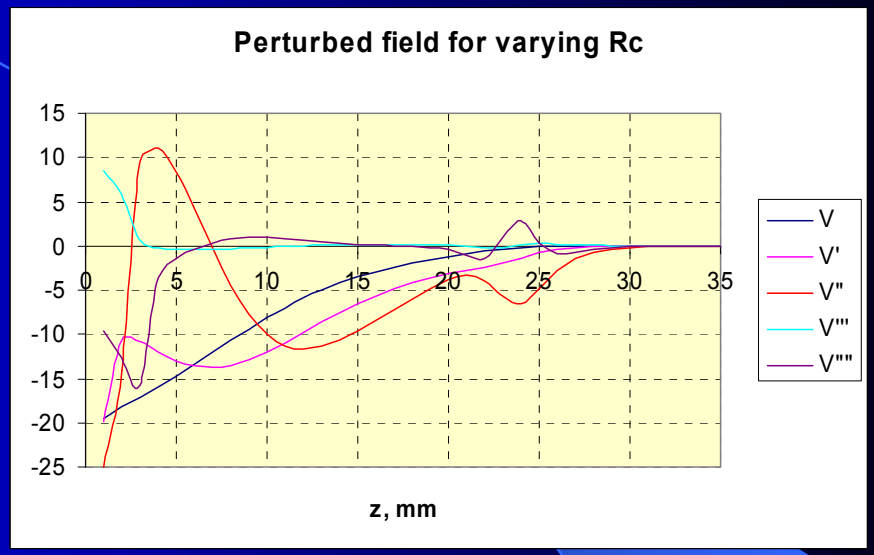

Tilt of the axis (m=1)

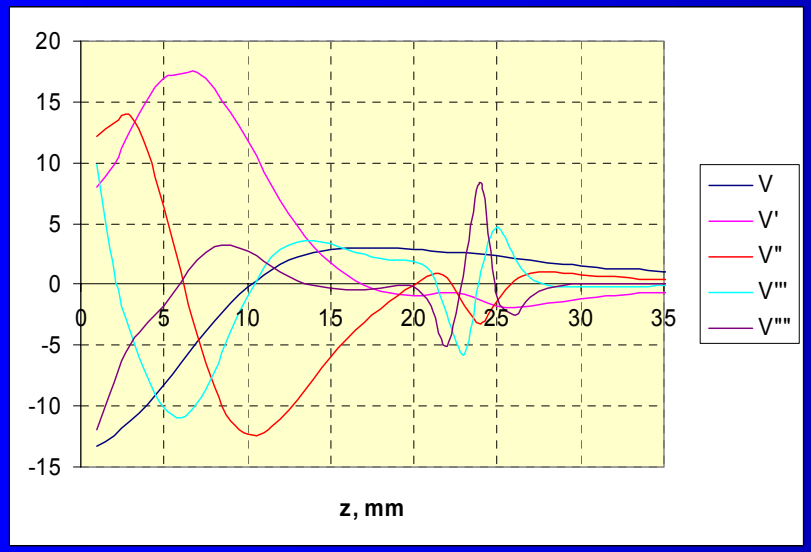

Elliptical deformation (m=2)

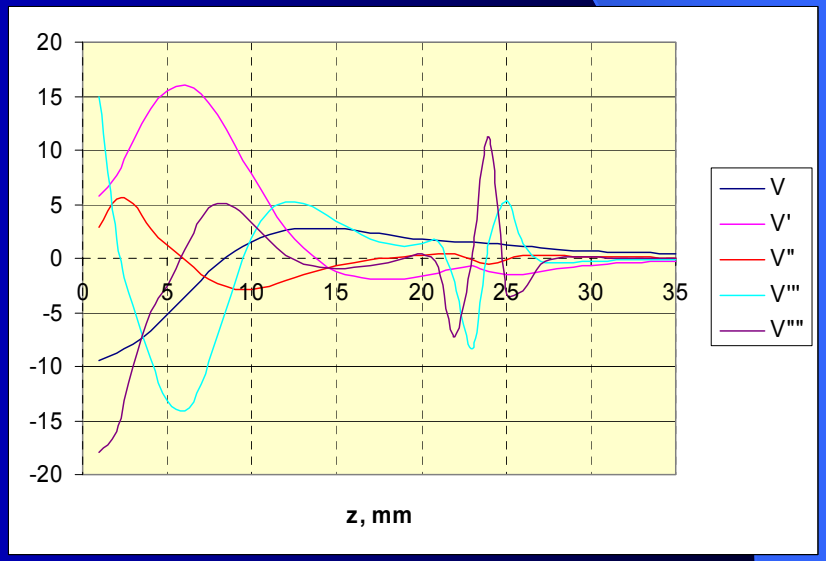

Numerical results for the tolerant defects a_i, mm

Resolution mm^{-1}	70	60	50		
Cathode dia, mm	18-80	18-80	18,25	40	80
a_1	0.01	0.03	0.05	0.07	0.08
a_2	0.04	0.1	0.2	0.02	0.17
a_3	0.04	0.1	0.2	0.02	0.17
a_4	0.007	0.02	0.03	0.03	0.04
a_5	0.01	0.04	0.06	0.08	0.1
a_6	0.1	0.2	0.4	0.5	0.7

Structural Synthesis

Classical approaches

1. Scherzer series
   Numerical instability;

$$\varphi(r,z)=\sum_{i=0}^{\infty}\frac{(-1)^i}{(i!)^2}\left(\frac{r}{2}\right)^{2i}\Phi^{(2i)}(z),\qquad \Phi(z)\equiv\varphi(0,z)$$

2. Conformal mapping
   Mapping singularity;

$$\varphi(r,z)=\frac{1}{2\pi}\int_0^{2\pi}f(z+ir\cos\alpha)d\alpha.$$

3. Finite-difference approximation for the Cauchy problem.
   Numerical instability;
4. No additional requirements (like constraint functionals F_j);
5. No tolerance analysis.

The ideal analytical model and the practical Pierce gun

$$\varphi(r,z) = C(r^2 + z^2)^{2/3} \cos\left(arctg\ \frac{r}{\ }\right)$$

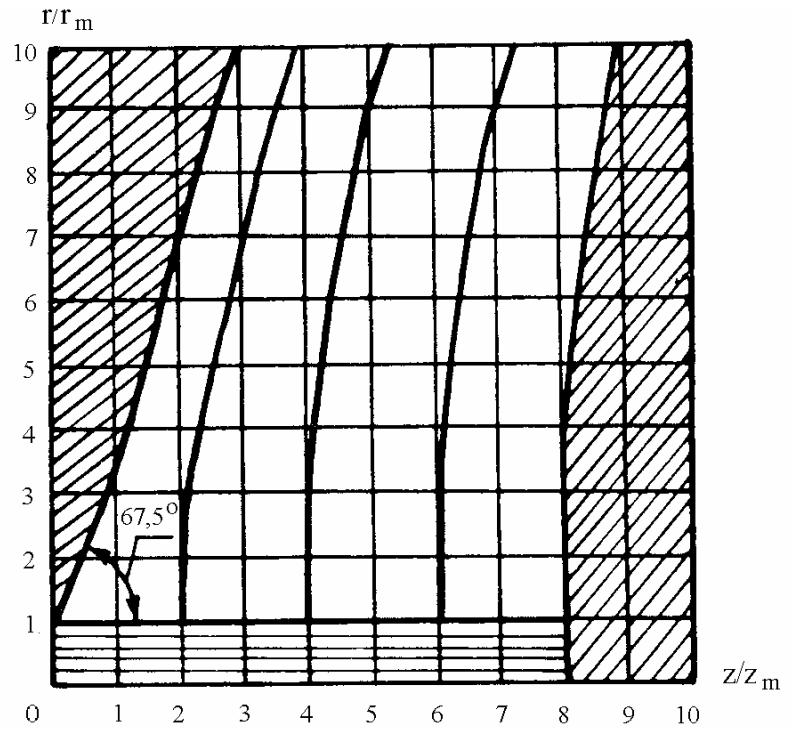

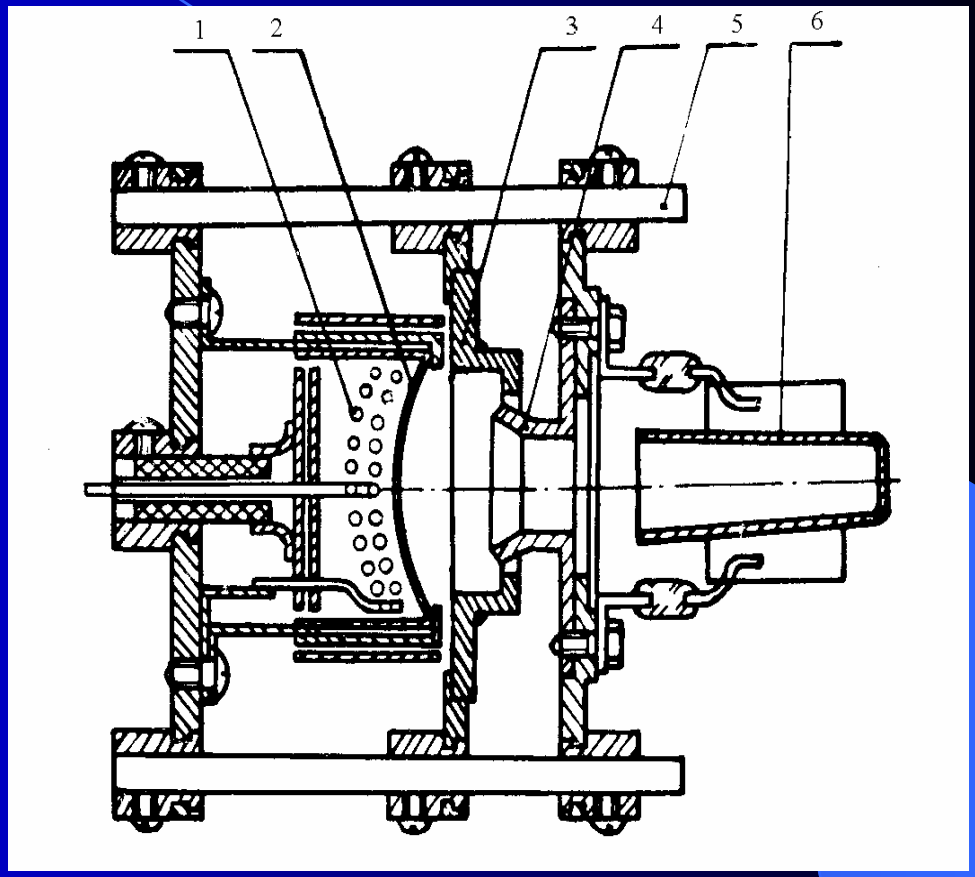

1- heater; 2 – cathode; 3 – focusing electrode; 4 – anode; 5 – ceramic insulator; 5 – collector.

The results of classical approach

The absence of technical constraints in classical synthesis produces the solutions unrealizable in practical manufacturing.

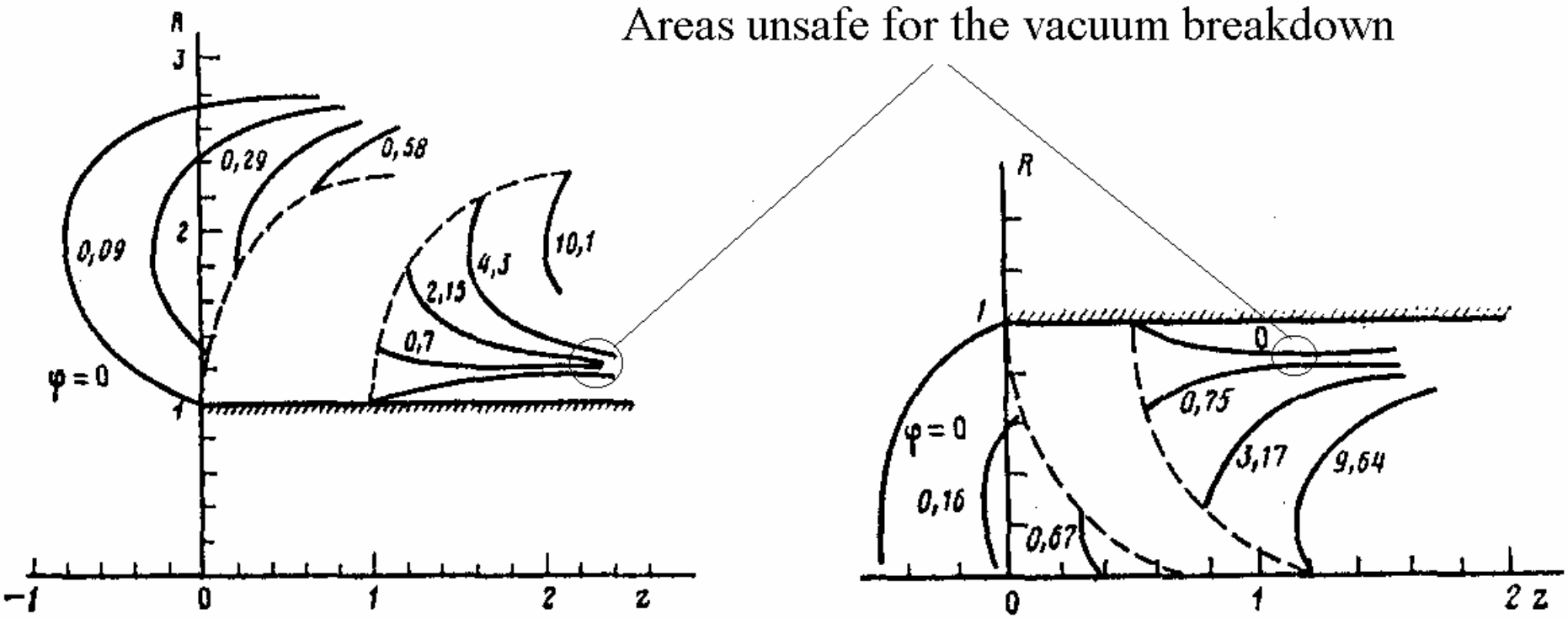

New formulation of the synthesis problem is suggested

1. Obtain the Cauchy data $\Phi(z)$ by minimizing the objective functional $F_{0;}$
2. Introduce 3 types of surfaces: a) fixed-shape electrodes with the boundary conditions; b) surface with the Cauchy data and c) “skeleton” surface with the field sources (charges, dipoles).
3. Determine the field source values from the solution of mixed boundary/Cauchy problem;
4. Obtain the electrode shape from the map φ_i=c;
5. Obtain the real shape in the “tolerance range”.

Algorithms of BEM

Boundary conditions

$$\left(\alpha\varphi + \beta\frac{\partial\varphi}{\partial n}\right)_S = \psi(s),$$

Cauchy data on the axis

$$\varphi\big|_{S0} = \Phi(\tau),$$

Integral equations (mixed formulation)

$$\psi(s) = \int_{\Gamma+S}\sigma(t)\left[\alpha + \beta\frac{\partial}{\partial n}\right]G_\sigma(s,t)d\Gamma + 2\pi\sigma(s) +$$

$$\int_\Gamma \nu(t)\left[\alpha + \beta\frac{\partial}{\partial n}\right]G_\nu(s,t)d\Gamma + 2\pi\nu(s),$$

$$\Phi(\tau) = \int_{\Gamma+S}\sigma(t)G_\sigma(s,t)d\Gamma + \int_\Gamma \nu(t)G_\nu(s,t)d\Gamma + 2\pi\nu(s).$$

Approximation and linear system

$$X \equiv \begin{bmatrix} \sigma \\ \nu \end{bmatrix}, \quad F \equiv \begin{bmatrix} \psi \\ \Phi \end{bmatrix},$$

Source approximation with cubic spline

$$X(t) = M_{i-1}\frac{(t_i - t)^3}{6h_i} - M_i\frac{(t_{i-1} - t)^3}{6h_{i-1}} + (X_{i-1} - M_{i-1}\frac{h_i^2}{6})\frac{t_i - t}{h_i} - (X_i - M_i\frac{h_i^2}{6})\frac{t_{i-1} - t}{h_i}.$$

Green functions (single & double layer potentials)

$$G_\sigma = \frac{r'K(k)}{\pi\varepsilon_0\delta}, \quad \delta^2 = (r + r')^2 + (z - z')^2,$$

$$G_\nu = \frac{1}{\pi\varepsilon_0\delta}\left\{\frac{r'}{2r}\left[\frac{(r')^2 - r^2 + (z - z')^2}{\delta}E(k) - K(k)\right]\cos(\vec{n}\vec{e}_r) + \frac{r'(z - z')E(k)}{(r - r')^2 + (z - z')^2}\cos(\vec{n}\vec{e}_z)\right\}.$$

Linear Problem in weak formulation

$$\Re = (X^* G^* - F^*)D(GX - F) \to \min$$

The Synthesis of Matching Lenses

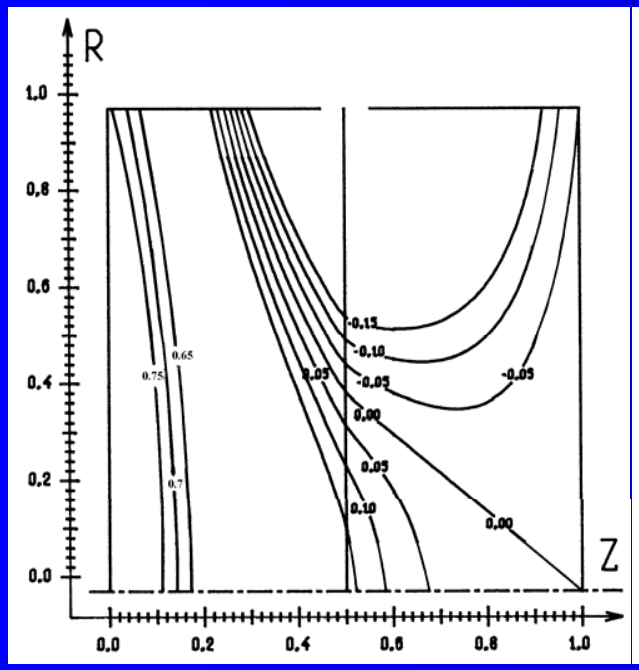

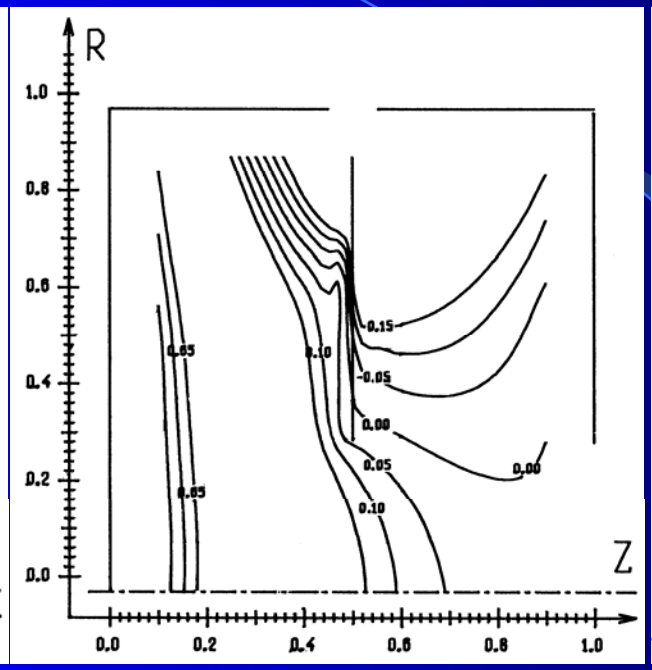

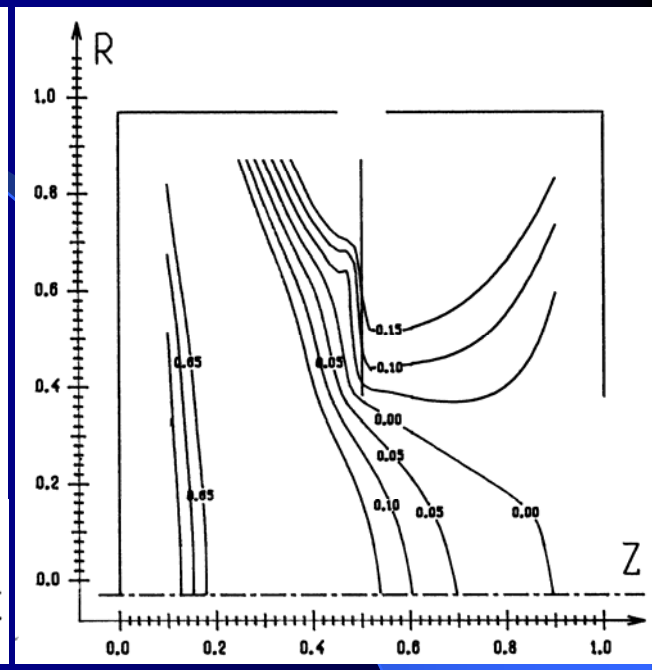

Ideal lens | Aperture hole a=0.3 | Aperture hole a=0.4

Critical aperture:

$$a_0 = \sqrt{2/3}(1-\lambda_0) \approx 0.4463.$$

The Synthesis of Single Lens

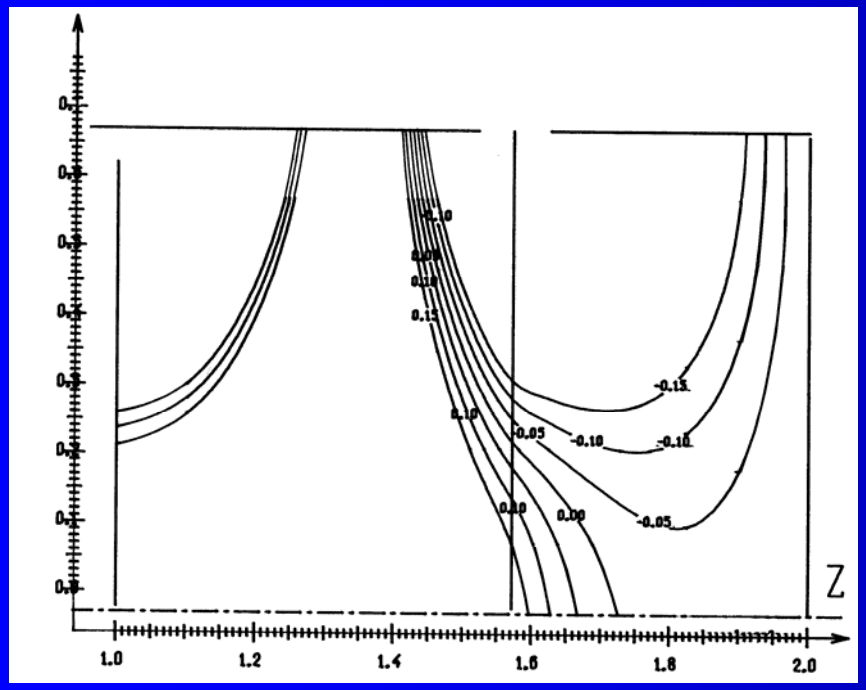

Ideal Lens

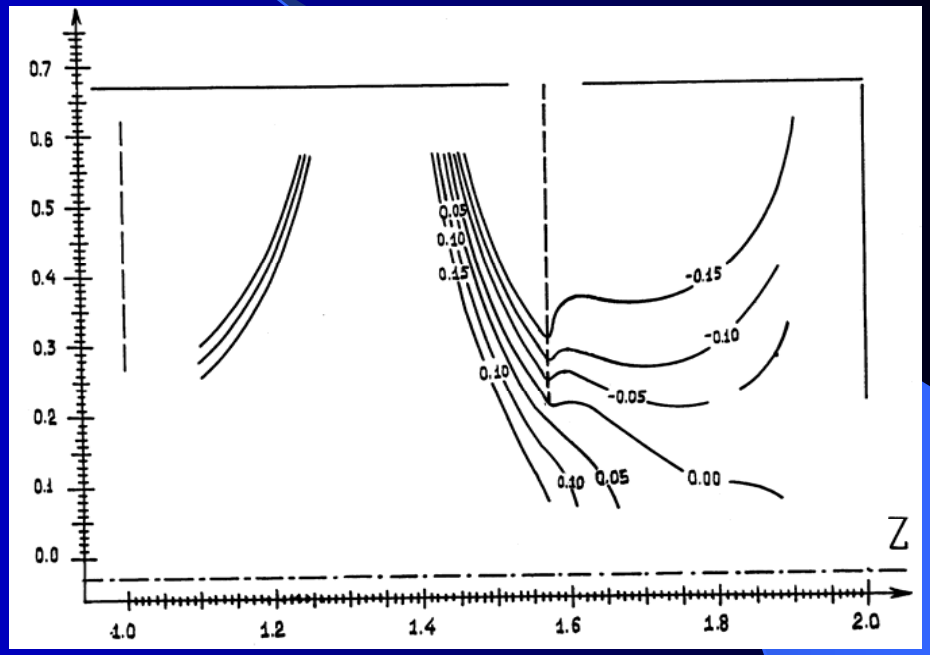

Aperture hole a=0.25

The Butler Lens Forming an Ideal Cylindrical Beam

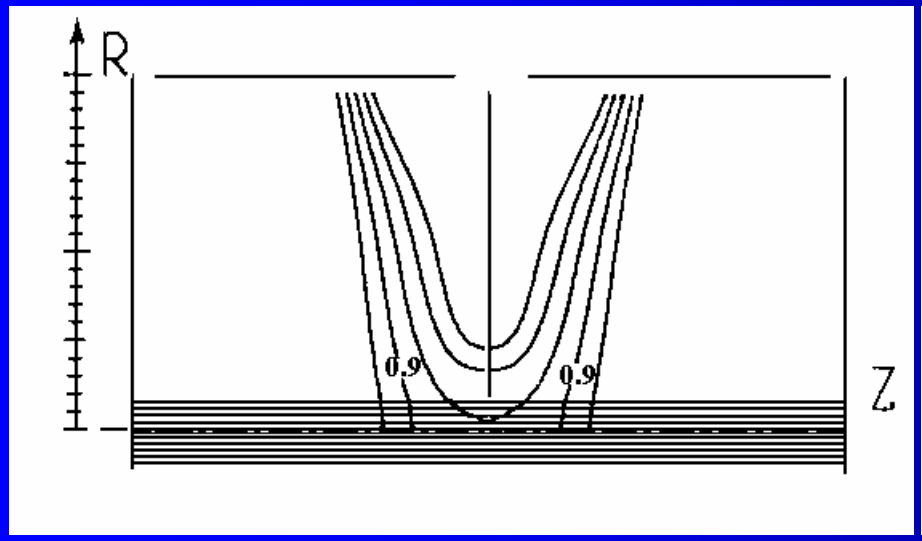

W = 0.09

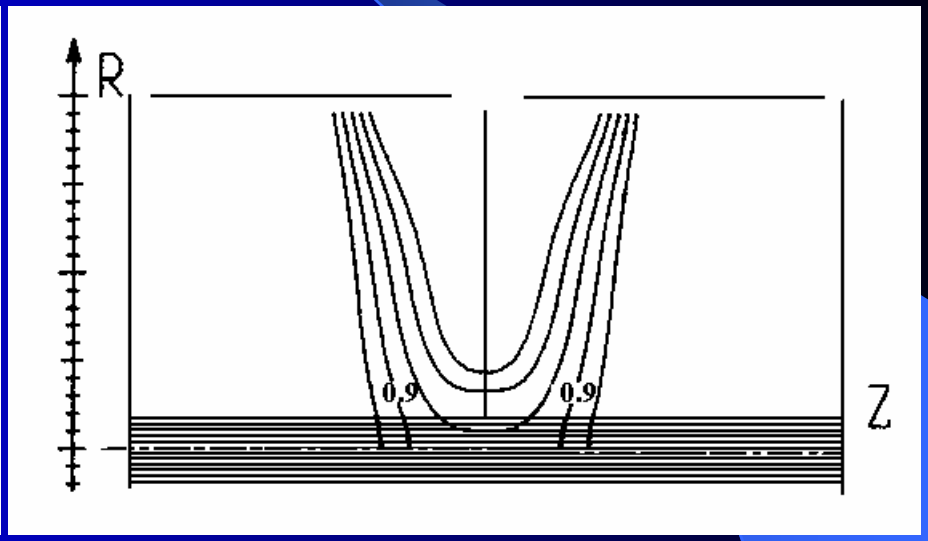

W = 0.2

Beam parameters : U=4KeV; P=0.55μA/$V^{3/2}$

Summary

- New approaches in formulation for complex problems of analysis, optimization and synthesis are suggested;
- Set of precision methods and algorithms are implemented. Their effectiveness was demonstrated for different application areas;
- The numerical tools and computer codes for 2D and 3D problems are successfully used in practical design during more than 30 years. Many unique devices have been constructed using numerical design.